JOURNAL OF GEOPHYSICAL RESEARCH, VOL. 103, NO. B4, PAGES 7211-7229, APRIL 10, 1998

Transition from oblique subduction to collision: Earthquakes in the southernmost Ryukyu arc–Taiwan region

Honn Kao

Institute of Earth Sciences, Academia Sinica, Taipei, Taiwan

Sern-su Jack Shen and Kuo-Fong Ma

Institute of Geophysics, National Central University, Chung-Li, Taiwan

Abstract. Tectonic characteristics of the region between Taiwan and the southernmost Ryukyu arc are inferred from a detailed analysis of local seismicity and source parameters of 62 recent earthquakes of $5.5 \le m_b \le 6.6$. Five major seismogenic structures can be delineated: the Collision Seismic Zone (CSZ), the Interface Seismic Zone (ISZ), the Wadati-Benioff Seismic Zone (WBSZ), the Lateral Compression Seismic Zone (LCSZ), and the Okinawa Seismic Zone (OSZ). In the CSZ, located along the east coast of Taiwan and offshore, earthquake focal mechanisms show horizontal P axes distributed in two directions, 287°±10° and 333°±16°, possibly reflecting a strain partition associated with the relative plate convergence between the Eurasia plate and the Philippine Sea plate. The corresponding seismic strain tensor indicates a maximum compressive strain rate of 1.2×10^{-7} yr^{-1} along 293° and a comparable extension in vertical direction, presumably resulted from plate collision in the region. The geometry of the ISZ, which is distorted significantly at its westernmost end, can be approximated by a north dipping plane that is gradually pushed northward with increasing dip. The seismogenic portion of the interface spans a short depth range from ~10 km to ~35 km. A clear pattern of earthquake slip partition is observed; the average slip vector residual is as large as 35°. Seismic strain patterns within the subducted Philippine Sea slab show predominantly downdip extension between 80 and 120 km and downdip compression at ~270 km, different from the pattern of strain segmentation observed for the rest of the Ryukyu arc where the northern and southern portions are dominated by downdip extension and compression, respectively. Owing to the large convergence obliquity, the slab is descending at a rate significantly slower near Taiwan than in the southern Ryukyu. Thus we interpret the appearance of downdip extension within the subducted lithosphere as a combined result of oblique subduction and the slab's negative buoyancy. A number of thrust or oblique strike-slip earthquakes between ISZ and WBSZ show a consistent pattern of lateral compression with P axes oriented roughly parallel to the local strike of the trench-arc system. They are probably due to the compressive strain originated from the collision and transmitted laterally within the lithosphere. Shallow normal-faulting earthquakes show successive rotation of T axes from approximately N–S in the Okinawa trough to approximately E–W in northeast Taiwan, possibly as a result of interaction between the extension from the opening of the Okinawa trough and the compression from collision. One normal event (January 18, 1991, m_b=5.9) occurred in the Central Range with T axis roughly parallel to the structural trend of Taiwan, implying that the nature of the orogeny in Taiwan has changed from "thin-skinned" deformation to lithospheric collision involving the whole crust and uppermost mantle.

1. Introduction

The oblique subduction is common in the circum-Pacific [*Fitch*, 1972; *Jarrard*, 1986a, b; *DeMets et al.*, 1990]; it is particularly complex near Taiwan due to its unique tectonic setting. Two subduction zones, the Ryukyu trench and the Manila trench, are located to the northeast and south of Taiwan, respectively (Figure 1) [e.g., *Wu*, 1978; *Tsai*, 1986].

Paper number 97JB03510.
0148-0227/98/97JB-03510 $09.00

The Philippine Sea plate moves northwesternly and subducts beneath the Eurasia plate along the Ryukyu trench but overrides the Eurasia plate along the Manila trench (Figure 1). The trench normal directions along most of the Ryukyu arc stay within 20° of the relative plate convergence, except to the west of 127°E where the strike of the trench gradually changes from NE–SW to almost E–W [e.g., *Fitch*, 1972; *Liu et al.*, 1995]. Furthermore, the morphology of the trench disappears to the west of 123°E where it is intercepted by the Gagua Ridge (Figure 1). Similarly, the Manila trench system, which has a trench normal in approximately E–W direction, is obliquely oriented to the relative plate convergence (Figure 1). To the north of 21.5°N, the Manila trench–Luzon arc

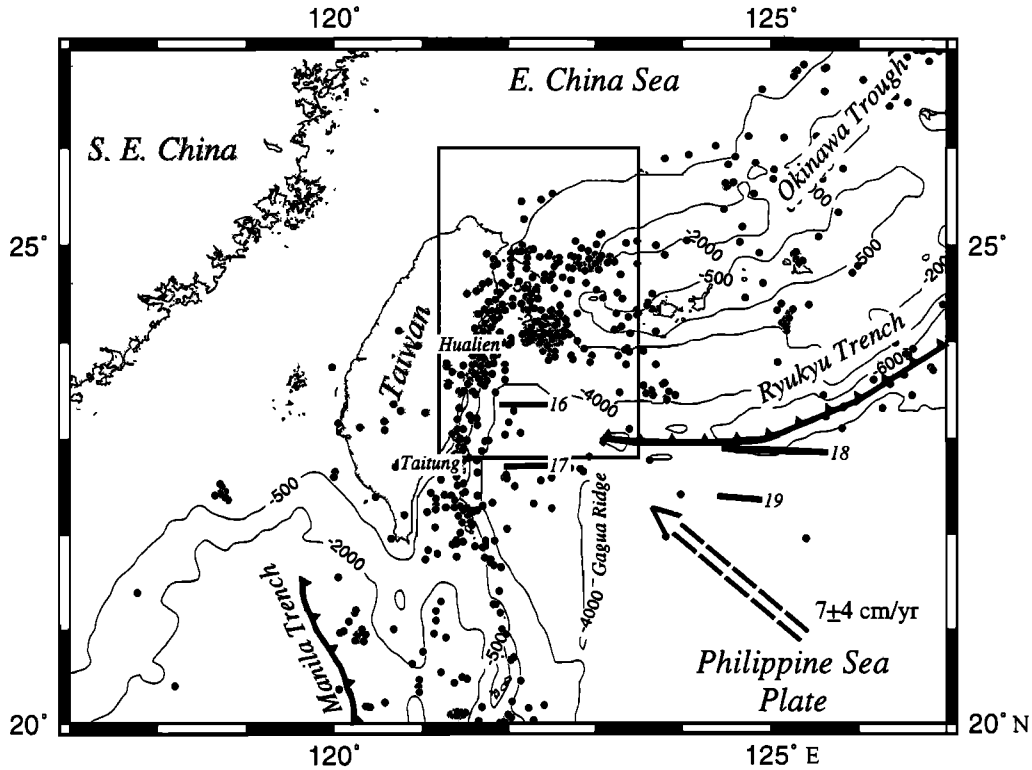

Figure 1. Bathymetry and seismicity of $m_b \geq 5.0$ (solid circles) between 1964 and 1995 in the southernmost Ryukyu arc–Taiwan region. The Philippine Sea plate is moving NW at 7±4 cm yr^{-1} relative to the Eurasia plate, creating the Taiwan Collision Zone. The Longitudinal Valley between Hualien and Taitung is believed to be the suture. Morphology of the Ryukyu trench disappears to the west of 123°, where it is intercepted by the Gagua Ridge. Magnetic anomaly chrons 16 and 17 and 18 and 19 (solid straight lines) are found to the west and east of the Gagua Ridge, respectively. To the south of Taiwan is the Manila trench system, whose bathymetric signature disappears to the north of ~21.5°N. The box shows our study area.

system gradually loses its bathymetric identity as it encounters the continental margin of the SE China.

The collision in Taiwan is a major tectonic event in the region for the past 4 Myr [e.g., *Ho*, 1988; *Teng*, 1990; *Lee and Lawver*, 1994]. The associated orogeny results in numerous earthquakes and many distinct geological features both on and off the island. Although it is generally accepted that the northwestern movement of the Luzon arc is ultimately responsible for the collision, exactly how the collision evolved into today's configuration is still under vigorous debate [e.g., *Suppe*, 1981, 1984; *Angelier et al.*, 1990; *Teng*, 1990; *Lu and Hsü*, 1992; *Lee and Lawver*, 1994; *Lu and Malavieille*, 1994; *Hsu and Sibuet*, 1995]. The present-day collision boundary is located along the Longitudinal Valley between Hualien and Taitung (Figures 1 and 2) that separates the Central Range to the west and the Coastal Range to the east [e.g., *Biq*, 1972; *Wu*, 1978; *Barrier and Angelier*, 1986; *Tsai*, 1986; *Ho*, 1986; *Salzberg*, 1995]. Whereas the Central Range is composed of rocks belonging to the passive margin of southeast Asia, the strata in the Coastal Range are mainly associated with the former Luzon arc [e.g., *Ho*, 1988]. The collision also caused significant clockwise rotation of major structures in northeast Taiwan [e.g., *Angelier et al.*, 1990; *Lu and Malavieille*, 1994; *Lue et al.*, 1995].

Seismicity in the region shows significant spatial variation (Figure 1). It is apparent that larger earthquakes ($m_b \geq 5.0$) occurred much more frequently near Taiwan than in typical trench–arc regions. Furthermore, earthquakes concentrate mostly along the east coast and northeast offshore. Such a pattern presumably reflects active collision between the Philippine Sea and the Eurasia plates, but exactly how the various structures in subduction zones transform into structures representing collision is largely unknown.

To further complicate the picture, the backarc basin of the Ryukyu trench, namely, the Okinawa trough (Figure 1), is in the process of opening and shows various extensional features, such as grabens and en échelon structures identified from regional bathymetry and seismic reflection profiles [e.g., *Herman et al.*, 1978; *Kimura*, 1985; *Sibuet et al.*, 1987; *Sato et al.*, 1994], earthquake focal mechanisms showing extensional faulting [e.g., *Shiono et al.*, 1980; *Eguchi and Uyeda*, 1983; *Kao and Chen*, 1991], high hydrothermal anomalies [e.g., *Lu et al.*, 1981; *Yamono et al.*, 1986; *Kimura et al.*, 1988], and thin crust with low Q values [e.g., *Ouchi and Kawakami*, 1989]. The extension may extend westward beneath northeast Taiwan, as suggested by some geodetic and tomographic studies [e.g., *Yeh et al.*, 1989; *Liu*, 1995].

Although the Ryukyu–Taiwan–Luzon system was one of the original examples cited in the pioneer studies of oblique subduction [e.g., *Allen*, 1962; *Fitch*, 1972], there is, to our best knowledge, no comprehensive study addressing exactly how the two oblique subduction zones are connected to the Taiwan Collision Zone. The purpose of our study is, therefore, to delineate the configuration of plate boundaries and the associated seismogenic structures for the two

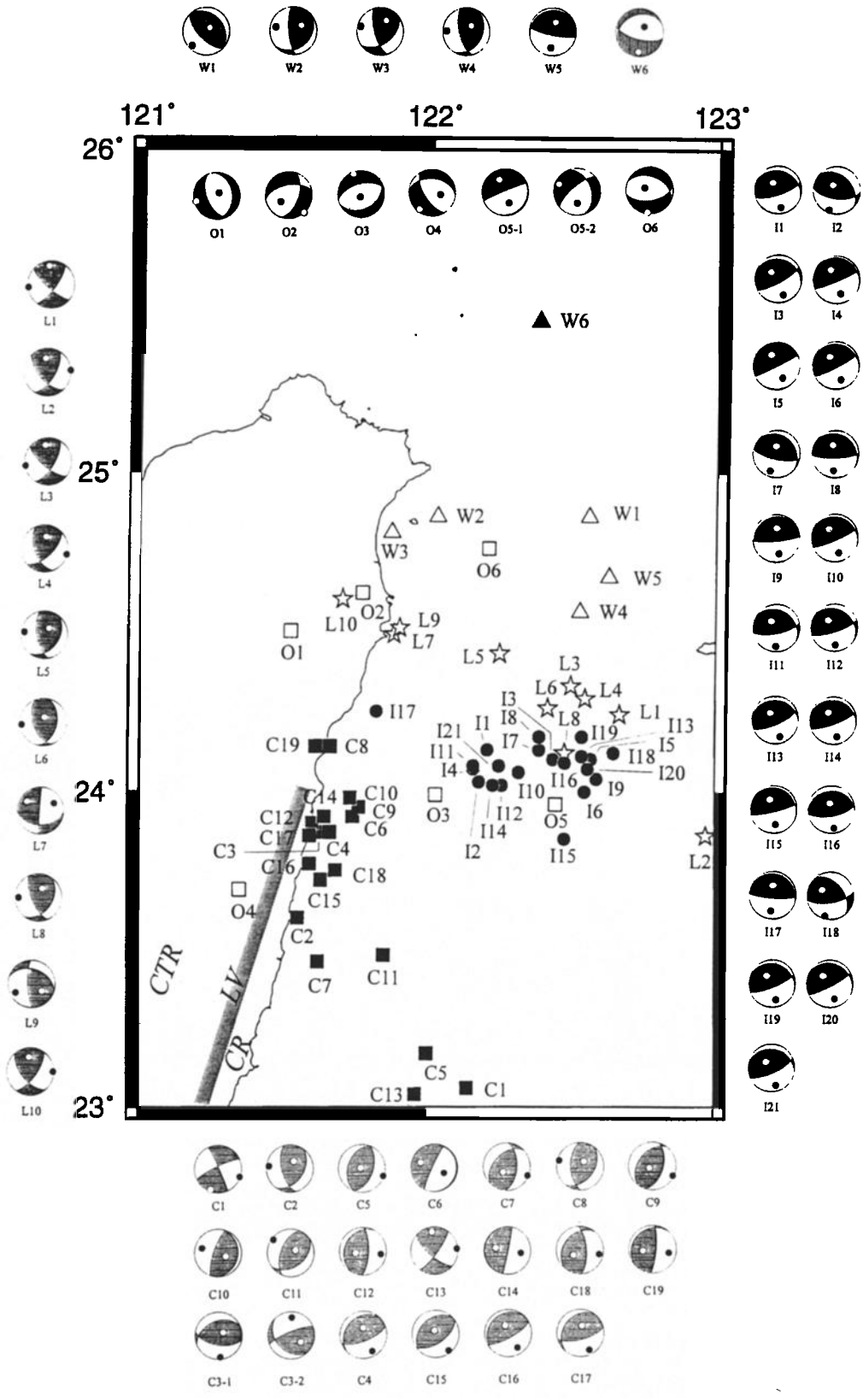

Figure 2a. Epicenters and focal mechanisms of earthquakes studied. Events are numbered according to Table 1. Equal-area projections of the lower hemispheres of the focal spheres for 62 earthquakes are plotted showing the orientation of the nodal planes, as well as that of the *P* (solid circles) and *T* axes (open circles). Shaded areas show quadrants with compressional *P* wave first motions. Five major seismogenic structures are delineated, as indicated by different symbols and shadings for epicenters and inside the shaded quadrants: Collision Seismic Zone (CSZ, solid squares), Interface Seismic Zone (ISZ, solid circles), Wadati-Benioff Seismic Zone (WBSZ) showing downdip extension (open triangles) and compression (solid triangle), Lateral Compression Seismic Zone (LCSZ, open stars), Okinawa Seismic Zone (OSZ) and normal-faulting earthquakes (open squares), respectively. The Central Range (CTR) and Coastal Range (CR) are located to the west and east, respectively, of the Longitudinal Valley (LV; shaded line). Second subevents are plotted if they are deemed significantly different from the first ones (e.g., events O5 and C3).

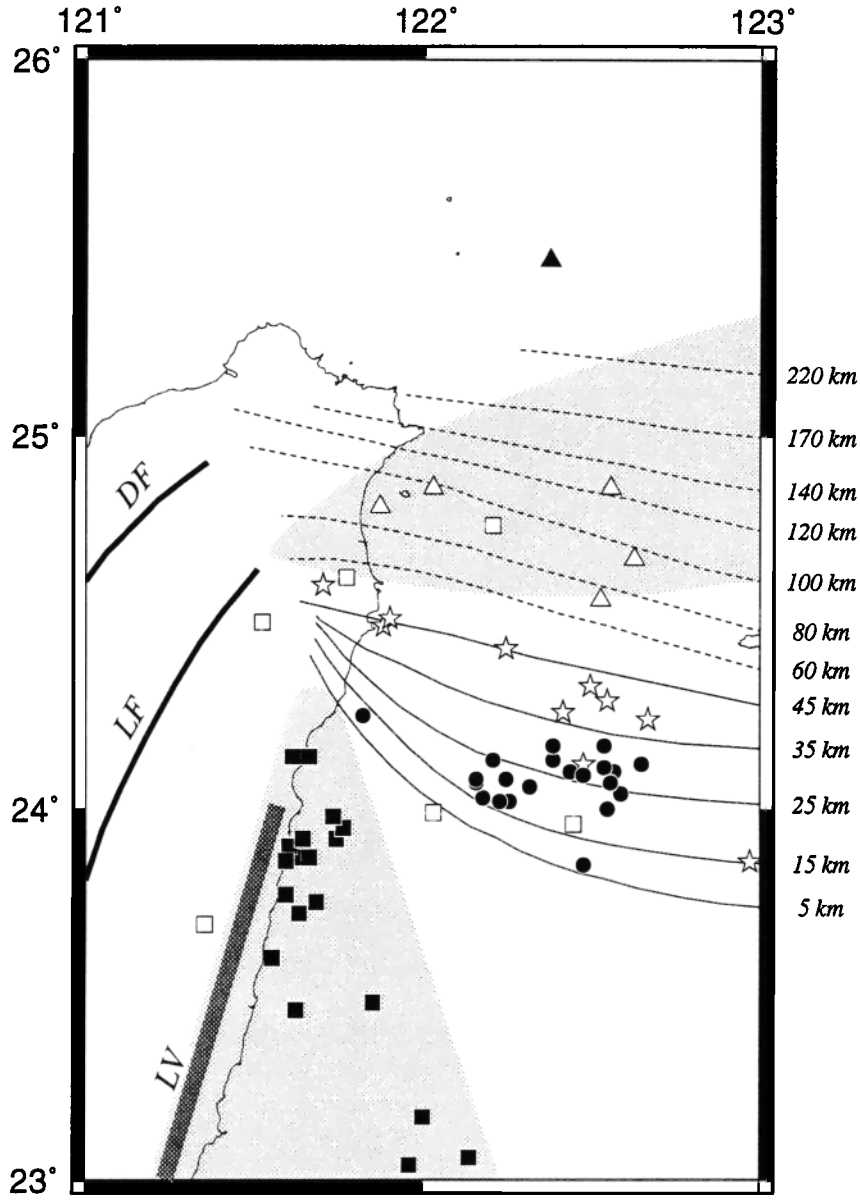

Figure 2b. Inferred configuration of seismogenic structures in the southernmost Ryukyu arc–Taiwan region. The CSZ (the large shaded triangular zone) is the predominant seismogenic structure in the region. The ISZ is significantly distorted at its westernmost end, as indicated by the solid isodepth contours between 5 and 45 km. The WBSZ is striking ~110° as shown by dashed isodepth contours of the top of the subducted slab. The LCSZ is located between ISZ and WBSZ from northeast Taiwan to the eastern edge of our study region. The OSZ (shaded area between ~24.5°N and ~25°N) extends westward into northeast Taiwan. Locations of the deformation front (DF) in west Taiwan and the Lishan fault (LF) are adapted from *Ho* [1988].

transition regions between Ryukyu and Taiwan and between Luzon and Taiwan. Given the different tectonic settings for the two regions (Figure 1), we focus the present paper only on the southernmost Ryukyu arc–Taiwan case and leave the Luzon–Taiwan case to a separate report.

We address the following issues specifically. What are the major seismogenic structures in the region? What are their characteristics and relationship to various tectonic processes? How do those structures differ from that observed along the rest of Ryukyu arc and along the Taiwan collision zone? Furthermore, how does the slip partition distribute in a region strongly affected by both collision and backarc opening? What is the response of the plate interface and the overriding plate to the oblique subduction? We also hope to gain insight to the geometrical configuration of the subducted Philippine Sea plate and the corresponding internal state of strain.

To answer these questions, we have systematically studied large and moderate-sized earthquakes in this region between 1964 and 1995, using seismic data from both local and global networks. The observed seismic patterns and the inferred slab configurations turn out to be very systematic. We find that distinct characteristics delineated from seismicity and focal mechanisms can be appropriately explained by regional tectonic processes and their interactions but are somewhat

different from what has been observed along the rest of the Ryukyu arc. We also find a prominent slip partition for the interface–forearc system and a pattern of strain partition for collision-related earthquakes east of Taiwan. On the basis of such findings, we attempt to construct a model to describe the present-day tectonic configuration in the region.

2. Seismicity, Seismogenic Structures, and Seismic Strain Patterns

A total of 62 earthquakes ($m_b \geq 5.5$) between 1964 and 1995 are included in this study (Table 1); 45 of them have good waveforms and acceptable azimuthal coverage for us to perform inversion. Source parameters (including focal depths, mechanisms, source time functions, seismic moments, source rupture velocity, and possible subevents) are determined by simultaneously inverting both *P* and *SH* waveforms recorded at teleseismic distances. The typical uncertainties are less than 13°, 7°, 15°, and 6 km for strike, dip, rake, and depth, respectively (Table 1). Some events, especially the subevents, may have larger values due to less constraints from waveforms. Readers are referred to *Nábelek* [1984] and *Kao and Chen* [1991, 1994, 1995] for technical aspects of the analysis. Source parameters for the remaining 17 events are adapted from previous studies (Harvard centroid-moment-tensor (CMT) solutions, *Dziewonski et al.* [1981], *Tsai et al* [1983], and *Pezzopane and Wesnousky* [1989]). The inversion results are summarized in Table 1 and Figure 2a and discussed briefly below; details are given in Appendix C[1] as an electronic supplement.

In Figure 3 we plot hypocenters of local events ($M_L \geq 3.0$) between 1990 and 1993 reported by the Seismological Observation Center of the Central Weather Bureau, Taiwan, to better define the regional seismic patterns and their relationship with respect to the configuration of both Philippine Sea and Eurasia plates. We show plots of horizontal slices at various depths to illustrate the distribution of hypocenters with respect to depth so that events associated with the subducted slab at intermediate depths can be easily distinguished from those associated with the opening of the Okinawa trough at shallow depths or with collision processes in east Taiwan. According to the number of earthquakes, the thickness of the slices is chosen to be 10 km above 50 km, 20 km between 50 and 150 km, 40 km between 150 and 190 km, and 60 km between 190 and 250 km.

In Figure 4 we show a cross section striking N15°E–S15°W to demonstrate the distribution of seismogenic structures associated with the subducted slab. On the basis of the distribution of hypocenters and characteristics of fault plane solutions, we are able to delineate five major seismogenic structures in the region: the Collision Seismic Zone (CSZ; events C1–C17), the Interface Seismic Zone (ISZ; events I1–I21), the Wadati-Benioff Seismic Zone (WBSZ; events W1–W6), the Lateral Compression Seismic Zone (LCSZ; events L1–L10), and the Okinawa Seismic Zone (OSZ; events O1, O2, and O6), as summarized in Figure 2 and discussed below.

To access the possible effect of epicentral mislocation on our results and interpretations, we have performed a Joint Hypocenter Determination (JHD [*Dewey*, 1972]) for 26 events (Appendix A) and compared the result to that reported by the International Seismological Centre (ISC) or Preliminary Determination of Epicenters (PDE). The location differences are less than 0.1° for most earthquakes studied. This is not surprising in view of the excellent focal coverage by global seismographic networks. However, the discrepancies between JHD locations and those determined using local data are somewhat larger, mainly because most of the events occurred outside the local network [*Tsai and Wu*, 1996].

2.1. Collision Seismic Zone (CSZ; Events C1-C17)

Collision between the Philippine Sea plate and Eurasia plate apparently plays an important role in the overall tectonics of the region [e.g., *Biq*, 1972; *Bowin et al.*, 1978; *Wu*, 1978; *Ho*, 1988; *Teng*, 1990; *Lee and Lawver*, 1994]. In terms of seismicity and fault plane solutions, the effect of collision could be recognized by earthquakes showing a consistent orientation of *P* axes in the collision direction [e.g., *Molnar and Tapponnier*, 1975; *Vilotte et al.*, 1982; *Fan et al.*, 1994; *Lukk et al.*, 1995]. Such a pattern is clearly identified in our results along the east coast of Taiwan and offshore, where all but two earthquakes exhibit predominately thrust faulting mechanisms (events C1 and C13 are strike-slip, Figure 2a). If we take 310° (i.e., N50°W [*Seno et al.*, 1993]) to be the direction of relative plate motion, then it is somewhat surprising to notice that only one event has its *P* axis located within ±10° of the convergence direction (event C11). For the rest, the orientation of *P* axes can be roughly divided into two groups: 287°±10° (i.e., N73±10°W; events C1, C2, C5–C14, C18, and C19; Figure 5a) and 333°±16° (i.e., N27±16°W; events C3, C4, C15–C17; Figure 5a). The number of the first group (showing approximately E–W compression) is about twice of the second group (showing N–S or NW–SE compression).

The focal depths of these events range from less than 10 km (events C4, C13–C16) to over 60 km (event C18), with more than half of them at depths shallower than 20 km and five took place between 30 and 40 km (Figure 5b). Such a bimodal depth distribution is similar to that observed for earthquakes in an intraplate (continental) setting [*Chen and Molnar*, 1983]. It probably reflects the variation of rheological strength with respect to depth, as discussed in section 3.

The distribution of local seismicity (Figure 3) reveals additional information about the geometry of CSZ. This structure is trending approximately N15±5°E with an average width of 30–35 km at the bottom but much wider at shallow depths, especially between 10 and 20 km. Most CSZ earthquakes deeper than ~50 km occurred at the northern end of the structure (Figure 3).

The vertical projection of CSZ does not coincide with the surface trace of the collision suture (i.e., the Longitudinal Valley, Figures 2 and 3) but is located to the east. The distribution of hypocenters in Figure 3 further suggests that the CSZ is steeply dipping to the east and that most collision-related seismic activity occurred within the Philippine Sea

[1]Supporting Appendix C figures are available on diskette or via Anonymous FTP from kosmos.agu.org, directory APEND (Username = anonymous, Password = guest). Diskette may be ordered from American Geophysical Union, 2000 Florida Avenue, N.W., Washington, DC 20009 or by phone at 800-966-2481; $15.00. Payment must accompany order.

Table 1. Summary of Source Parameters

Event[a]	Date	OT,[b] UT	Lat.,[b] °N	Lon.,[b] °E	Depth,[c] km	*P* Axis Az.,[d] Pl.,[d] deg	*T* Axis Az.,[d] Pl.,[d] deg	Strike, deg	Dip, deg	Rake, deg	m_b[b]	Seismic Moment, x10^{17} N m	Fig./Ref.[e]
					Collision Seismic Zone (CSZ)								
C1	Jan. 25, 1972	03:41:24.0	23.06	122.14	14	110, 4	201, 10	336	86	10	6.0	1340	PW89
C2	April 24, 1972	09:57:21.2	23.60	121.55	17(4.0)±4	277, 11	27, 61	36±11	41±4	132±6	6.1	164±23	C1
C3	Nov. 9, 1972	18:41:13.0	23.87	121.61	16(0.5)±4	177, 10	56, 71	100±6	57±3	109±5	5.9	12.5±4.2	C2
					2(0.5)±9	2, 25	125, 49	137±6	33±21	155±12		13.6±9.0	
C4	Nov. 21, 1972	02:47:16.4	23.87	121.66	8(1.0)±6	153, 22	357, 66	70±4	68±3	100±7	5.5	5.46±1.870	C3
					21(1.0)±10	144, 28	20, 47	78±12	80±7	121±28		1.60±0.80	
C5	Dec. 23, 1978	11:23:13.7	23.17	122.00	18	110, 5	290, 85	200	40	90	6.5	190	PW89
C6	Jan. 23, 1982	14:10:40.7	23.92	121.74	12(3.0)±7	119, 52	292, 38	205±4	83±4	-87±10	5.6	7.22±1.3	C4
C7	March 22, 1986	04:45:32.8	23.46	121.62	33	113, 6	216, 67	226	44	123	5.6	8.5	D87a
C8	May 20, 1986	05:25:48.4	24.14	121.66	22(1.0)±4	286, 8	38, 68	179±11	56±6	66±7	6.1	33.6±4.4	C5
					22(1.0)±5	122, 21	4, 49	169±18	37±9	27±13		9.83±3.73	
C9	Nov. 14, 1986	21:20:05.6	23.95	121.76	33(1.0)±8	117, 7	237, 78	17±6	52±3	77±4	6.1	1150±273	C6
C10	Jan. 6, 1987	05:07:48.1	23.98	121.73	38(1.0)±5	287, 29	114, 60	199±12	74±5	93±15	5.8	3.84±0.70	C7
					31(1.0)±9	231, 1	142, 48	175±16	58±11	141±18		2.59±0.70	
C11	April 24, 1988	20:03:29.2	23.48	121.85	41	307, 8	62, 71	202	55	69	5.5	1.7	D89
C12	July 20, 1988	23:15:36.7	23.90	121.60	36(1.0)±4	100, 25	258, 64	3±9	70±4	81±11	5.8	7.73±2.80	C8
C13	Aug. 3, 1989	11:31:20.4	23.04	121.96	9(3.5)±5	85, 5	353, 22	131±5	71±6	12±5	5.9	33.2±9.2	C9
C14	Dec. 13, 1990	03:01:48.0	23.92	121.64	6(1.0)±4	100, 42	284, 48	12±11	87±4	92±16	5.9	57.0±16.0	C10
C15	Dec. 13, 1990	19:50:17.9	23.72	121.63	10(1.0)±4	142, 11	345, 79	56±5	57±4	95±7	5.9	20.6±9.0	C11
C16	Dec. 25, 1990	14:21:53.2	23.77	121.59	8(0.5)±5	146, 27	340, 62	61±5	73±4	96±12	5.6	5.93±2.10	C12
					14(0.5)±10	128, 42	324, 46	45±10	88±6	98±23		1.94±0.84	
C17	April 19, 1992	18:32:00.2	23.86	121.59	14(0.5)±4	153, 20	13, 64	76±13	67±7	107±13	5.8	13.0±4.5	C13
C18	Sept. 1, 1992	16:41:13 4	23.75	121.68	63(2.0)±4	102, 19	234, 62	221±10	31±6	130±8	6.0	5.88±1.50	C14
C19	Feb. 23, 1995	05:19:01.9	24.14	121.61	34±4	103, 32	262, 56	5±6	78±4	80±11	5.9	11.8±1.4	C15
					Interface Seismic Zone (ISZ)								
I1	Jan. 13, 1968	07:03:45.8	24.13	122.21	27(3.3)±4	172, 26	321, 60	71±4	73±3	76±7	5.7	17.2±1.8	C16
I2	Feb. 16, 1971	14:26:10.8	24.03	122.18	24±5	202, 11	321, 68	96±5	59±4	68±6	5.7	5.53±0.48	C17
I3	April 17, 1972	10:49:44.4	24.10	122.44	22(4.0)±4	164, 30	312, 55	62±5	77±3	74±7	5.8	14.4±2.0	C18
					15(4.0)±6	187, 25	307, 48	72±5	77±4	57±7		8.93±2.0	
I4	July 15, 1977	02:12:56.6	24.07	122.16	15	164, 38	328, 50	67	84	82	5.6	6.8	D87b
I5	Feb. 8, 1978	00:15:40.5	24.10	122.57	15	154, 42	334, 48	64	87	90	5.5	14	D87c
I6	March 14, 1978	20:32:16.9	24.00	122.55	15	161, 36	323, 52	63	82	81	5.5	6.7	D87c
I7	June 21, 1983	14:48:07.9	24.13	122.39	24(4.0)±5	202, 24	353, 63	102±6	70±6	78±10	5.8	26.4±5.0	C19
					24(4.0)±9	215, 3	123, 43	161±9	63±10	145±14		17.3±8.5	
I8	June 24, 1983	09:06:46.3	24.17	122.39	30(4.0)±4	187, 30	343, 58	88±8	76±5	79±12	6.0	104±14	C20
					31(4.0)±7	178, 37	6, 53	91±13	82±7	94±19		20.0±8.0	
I9	June 25, 1983	19:40:54.0	24.04	122.59	14	172, 35	0, 55	85	80	94	5.5	1.74	D83
I10	Sept. 7, 1983	23:11:59.4	24.06	122.32	10	166, 35	325, 53	67	81	80	5.5	2.65	D84
I11	Sept. 21, 1983	19:20:44.4	24.08	122.16	21(3.0)±5	183, 24	321, 60	78±6	71±3	71±12	6.0	28.9±3.3	C21
I12	Sept. 23, 1983	12:29:23.4	24.02	122.26	19(3.0)±6	177, 27	318, 56	72±5	75±4	71±11	5.8	3.93±0.44	C22
					44(3.0)±12	95, 21	350, 34	40±11	82±7	139±17		3.10±0.60	
I13	March 28, 1984	09:11:21.0	24.11	122.54	35(4.0)±9	164, 28	321, 60	66±6	74±5	80±11	5.5	7.97±1.01	C23
I14	Feb. 27, 1986	06:23:13.3	24.02	122.23	15	167, 31	326, 57	69	77	80	5.8	5.7	D87a
I15	Feb. 12, 1988	19:15:35.4	23.85	122.48	21(4.0)±11	175, 37	336, 51	76±8	82±8	81±17	5.6	1.40±0.32	C24
I16	Aug. 21, 1989	23:12:41.4	24.09	122.48	19(3.0)±5	171, 22	342, 68	78±4	67±3	86±5	5.6	25.7±7.0	C25

Table 1. (continued)

Event[a]	Date	OT,[b] UT	Lat.,[b] °N	Lon.,[b] °E	Depth,[c] km	*P* Axis Az.,[d] Pl.,[d] deg	*T* Axis Az.,[d] Pl.,[d] deg	Strike, deg	Dip, deg	Rake, deg	m_b[b]	Seismic Moment, x10^{17} N m	Fig./Ref.[e]
I17	July 16, 1990	19:14:51.7	24.25	121.82	9(1.0)±6	187, 34	358, 56	296±20	12±6	112±20	5.5	2.84±1.20	C26
I18	Sept. 28, 1992	14:06:02.6	24.12	122.65	19(3.0)±5	198, 13	305, 54	323±10	44±5	143±6	5.8	12.0±2.70	C27
					19(3.0)±5	138, 22	342, 66	211±19	24±6	67±16		11.0±2.6	
I19	May 23, 1994	05:36:01.6	24.17	122.54	32(3.0)±3	168, 31	323, 56	68±14	77±7	78±14	5.7	12.7±4.4	C28
I20	May 23, 1994	15:16:57.1	24.07	122.56	21(3.0)±4	163, 35	317, 52	62±4	81±3	77±8	6.0	5.16±1.0	C29
					35(3.0)±2	171, 27	318, 59	69±7	74±5	75±11		4.12±1.60	
I21	April 3, 1995	11:54:43.6	24.08	122.25	24	166, 26	315, 61	65	72	76	5.7	3.7	D96
						Wadati-Benioff Seismic Zone (WBSZ)							
W1	July 1, 1966	05:50:38.0	24.86	122.56	110(0.5)±4	225, 17	44, 73	135±8	62±4	90±8	6.1	46.4±5.37	C30
W2	Oct. 9, 1971	13:15:38.5	24.86	122.03	95±8	282, 25	57, 56	175±8	73±6	68±10	5.7	3.72±0.42	C31
W3	Sept. 2, 1978	01:57:34.2	24.81	121.87	88	284, 14	29, 46	54	47	152	6.0	80	PW89
W4	Dec. 17, 1982	02:43:03.8	24.56	122.53	80(2.0)±7	272, 17	40, 64	29±10	33±6	128±8	5.9	4.40±0.9	C32
W5	April 26, 1983	15:26:40.2	24.67	122.63	115(2.0)±5	186, 33	17, 56	101±4	78±4	95±7	5.7	6.03±0.34	C33
W6	Feb. 13, 1984	04:48:57.7	25.47	122.38	269(4.0)±9	39, 64	183, 22	104±16	69±9	-75±17	5.5	2.35±1.50	C34
						Lateral Compressional Seismic Zone (LSZ)							
L1	March 12, 1966	16:31:19.9	24.24	122.67	22	263, 2	354, 23	36	73	165	6.6	4860	PW89
L2	March 23, 1966	00:04:33.4	23.86	122.97	45(4.0)±4	85, 1	354, 42	31±5	63±3	147±4	6.3	27.5±1.9	C35
L3	May 5, 1966	14:21:22.3	24.33	122.50	40	259, 1	350, 31	129	70	24	5.6	-	T83
L4	May 28, 1966	00:03:59.2	24.29	122.55	44(0.5)±5	104, 5	9, 48	46±5	62±6	139±7	5.5	6.30±0.49	C36
L5	Oct. 25, 1967	00:59:23.3	24.43	122.25	58(2.0)±5	278, 14	36, 62	37±3	37±3	132±5	6.0	205±44	C37
L6	Nov. 27, 1970	09:39:24.1	24.26	122.24	49(1.5)±6	261, 6	7, 69	11±13	42±10	115±14	5.7	3.94±0.80	C38
L7	Jan. 29, 1981	04:51:37.4	24.49	121.88	15	61, 35	304, 33	183	88	-128	5.7	10	D88
L8	Jan. 13, 1985	21:51:22.5	24.12	122.48	36	269, 15	22, 56	156	66	57	5.8	1.73	D85
L9	June 5, 1994	01:09:30.1	24.51	121.90	8(1.0)±4	242, 23	125, 47	178±5	76±4	125±9	6.1	32.8±14.0	C39
L10	June 25, 1995	06:59:06.2	24.60	121.70	47(1.0)±6	90, 6	355, 39	36±4	68±3	146±5	5.8	6.98±1.90	C40
						Okinawa Seismic Zone (OSZ) and Normal-Faulting Earthquakes							
O1	May 10, 1983	00:15:05.0	24.50	121.52	7(3.0)±4	36, 77	256, 10	159±11	55±8	-100±10	5.6	3.48±0.62	C41
					30(3.0)±7	38, 11	131, 15	174±17	72±9	177±14		2.19±0.80	
O2	July 30, 1986	11:31:48.9	24.62	121.77	14±5	230, 53	140, 0	19±16	56±9	-136±15	5.6	1.60±0.60	C42
					20±5	219, 76	28, 14	114±18	31±11	-95±16		1.39±0.60	
O3	April 11, 1987	18:13:28.3	23.99	122.03	14(2.0)±6	198, 79	340, 9	62±10	37±4	-102±7	5.6	5.96±0.90	C43
O4	Jan. 18, 1991	01:36:26.7	23.69	121.35	5±3	105, 60	218, 13	149±8	63±7	-60±11	5.9	3.70±0.98	C44
O5	May 24, 1994	04:00:42.1	23.96	122.45	35(3.0)±7	162, 49	334, 41	248±5	86±3	-86±10	6.2	36.5±9.6	C45
					10(3.0)±4	180, 49	293, 18	229±7	72±4	-53±7		34.9±6.2	
O6	Oct. 28, 1994	23:51:12.2	24.76	122.21	33	297, 72	186, 7	81	54	-111	5.5	3.3	D95

[a]Events are numbered in chronological order. Results for each subevent are given in successive rows.

[b]Epicenters (Lat., latitude; Lon., longitude), origin times (OT), and magnitudes are those reported in the *Bulletin of the International Seismological Centre* (ISC) and the Preliminary Determination of Epicenters (PDE) for events before and after 1988, respectively.

[c]Depth below sea level. Where applicable, the value inside parentheses is the thickness of the water column above the source region.

[d]Az., azimuth; Pl., plunge.

[e]Figure numbers in Appendix C or cited references. T83, *Tsai et al.* [1983]; PW89, *Pezzopane and Wesnousky* [1989]; D83, *Dziewonski et al.* [1983]; D84, *Dziewonski et al.* [1984]; D85, *Dziewonski et al.* [1985]; D87a, *Dziewonski et al.* [1987a]; D87b, *Dziewonski et al.* [1987b]; D87c, *Dziewonski et al.* [1987c]; D88, *Dziewonski et al.* [1988]; D89, *Dziewonski et al* [1989]; D95, *Dziewonski et al.* [1995]; D96, *Dziewonski et al.* [1996].

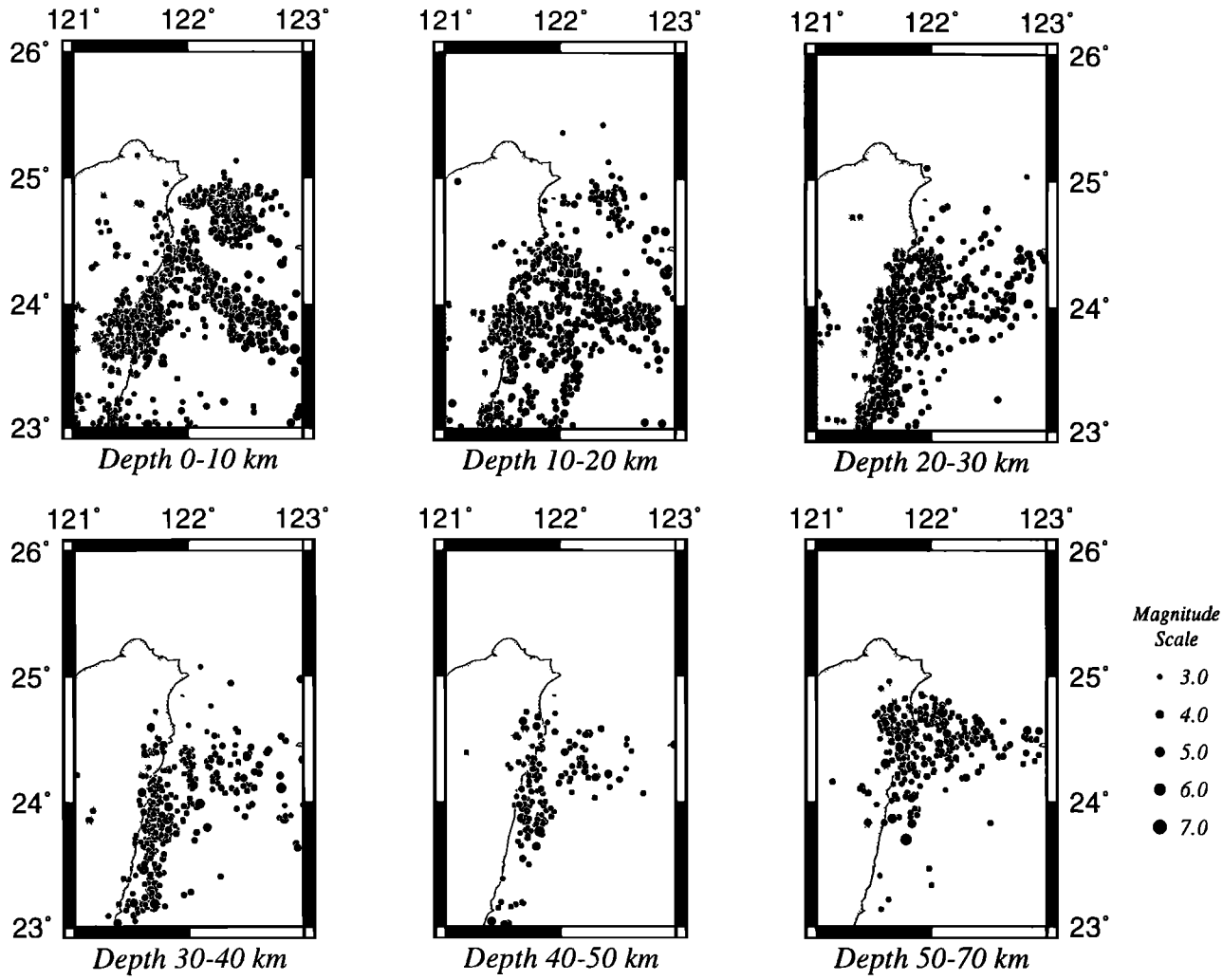

Figure 3. Seismicity ($M_L \geq 3.0$) during 1990–1993 in the study area as reported by the Seismological Observation Center of the Central Weather Bureau, Taiwan. Earthquake hypocenters in different depth ranges are shown in separate plots. At shallow depths, most events are associated with the collision zone, the plate interface, and the opening of the Okinawa trough, whereas at intermediate depth the seismicity clearly outlines the geometry of the subducted Philippine Sea plate.

plate in front of the suture zone. The relative plate movement here probably involves both strike-slip and thrust components and is accomplished more by aseismic than seismic deformation across the Longitudinal Valley [e.g., *Angelier et al.*, 1997].

2.2. Interface Seismic Zone (ISZ; Events I1–I21)

Interface earthquakes usually show two characteristics. The hypocenters are aligned with a planar structure that presumably is the interplate thrust zone; the focal mechanisms show low-angle thrust faulting with one shallowly dipping nodal plane compatible with the plate interface inferred from hypocenters [e.g., *Isacks et al.*, 1968; *Kanamori*, 1970; *Kao and Chen*, 1991]. In this study, more earthquakes show low-angle thrust mechanisms than in any other groups (I1–I21, Figures 2 and 4), although earthquakes in the CSZ have more seismic moment release (3.1×10^{20} N m), indicating the dominance of both subduction and collision in controlling the seismogenic behavior of the region.

Most low-angle thrust events cluster between 24°N and 24.2°N and to the east of 122.1°E (Figure 2a) except event I17. As shown in Figure 3, the shallow (≤50 km) local earthquake hypocenters to the south of ~24.5°N roughly form a "Γ" shape that presumably is a combination of the CSZ (approximately N–S oriented) and the ISZ (approximately E–W oriented). With decreasing depth, the hypocenters in CSZ seem to maintain its approximately N–S trend whereas the distribution of ISZ hypocenters gradually turns from approximately E–W direction to NW–SE, such that the junction of CSZ and ISZ always remains in the vicinity of 24.4°N, 121.8°E. This seismicity pattern suggests that as the Ryukyu arc approaches Taiwan, the initially shallowly dipping plate interface progressively increases its dip such that its upper end (say, at 10 km) is pushed northward (Figure 2b). This pattern is consistent with our inversion result that the westernmost event (I17) of ISZ, located to the north of the northern terminus of CSZ just offshore of Taiwan, has the shallowest focal depth. We infer that the westernmost part of ISZ is probably distorted significantly from a shallowly

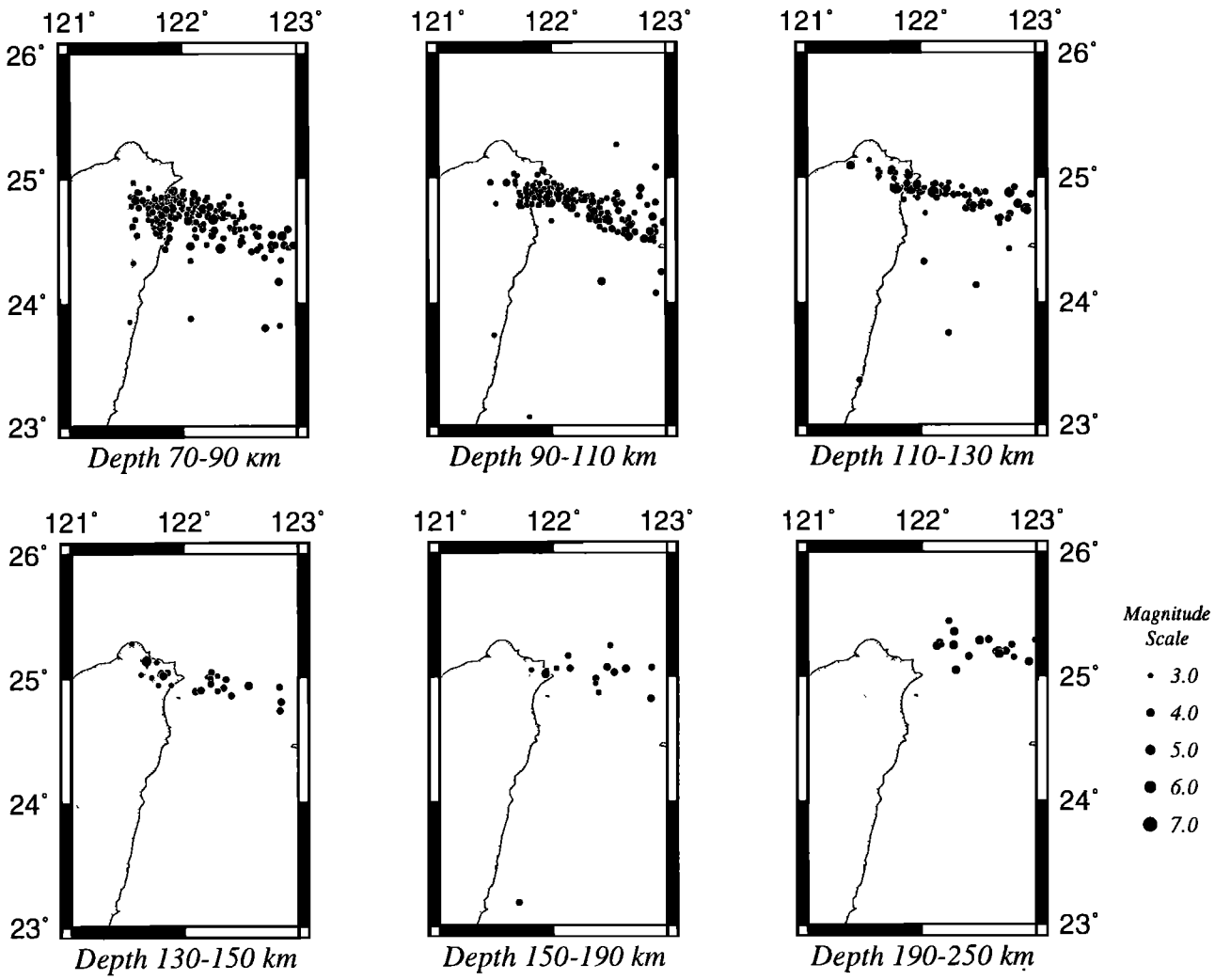

Figure 3. (continued)

dipping plane to being nearly vertical where it connects to CSZ (Figure 2b).

As shown in Figure 4, most ISZ events cluster around a plane dipping to the north with a depth range of ~10 km to ~35 km, which is shallower than observed along the rest of Ryukyu arc (~30–50 km [*Kao and Chen*, 1991]). It is also shorter than other subduction zones in the western Pacific such as the Kuril–Kamchatka arc (~15–50 km [*Kao and Chen*, 1994, 1995]) and the Japan arc (~15–45 km [*Kao and Chen*, 1996]).

We have noticed that events I2, I5, I13, I15, I17, and I18 do not fall exactly on the inferred plate interface and that the shallowly dipping nodal planes of events I2 and I18 are significantly steeper, whereas that of event 5 is nearly horizontal (Figures 2a and 4). Such deviations could be due to distortion or finite thickness of the ISZ (e.g., event I17), occurrence not exactly along the plate interface (events I2, I5, I13, I15, I18), or uncertainties in depths (e.g., events I5, I13, and I15).

2.3. Wadati-Benioff Seismic Zone (WBSZ; Events W1–W6)

Earthquakes deeper than ~70 km are mostly associated with a Wadati-Benioff zone [*Wadati*, 1927; *Benioff*, 1949, 1954] located within a subducted, presumably colder lithosphere. In our case, we found six events belonging to this structure at depths betweeen ~80 and ~270 km (Figure 4). Our waveform inversions indicate downdip extension for events W1–W5 and downdip compression for event W6, suggesting a transition of state of strain within the subducted slab somewhere between 120 and 260 km.

The dip angle of the subducted lithosphere can be estimated from the distribution of the hypocenters to be ~45–50° between 80 and 120 km and ~65° for depths below 120 km which is ~10° steeper than in the southern Ryukyu arc [e.g., *Kao and Chen*, 1991]. Similar increases of dip angle with depth are observed along many subduction zones [e.g., *Isacks and Barazangi*, 1977; *Bevis and Isacks*, 1984].

The strike of WBSZ, on the other hand, is better defined by local seismicity in Figure 3. For all depths below 70 km, the hypocenters clearly distribute along a structure striking N70±10°W. If we take the trench normal direction to be perpendicular to the strike of the WBSZ, then the "convergence obliquity", ϕ (i.e., the angle between the direction of plate convergence, N50°W, and trench normal) is as large as 70±10° (Figure 6). Thus much of the plate motion is in the lateral direction. Indeed, the vertical descending rate has been estimated to be only ~2.2 cm yr^{-1} for the subducted

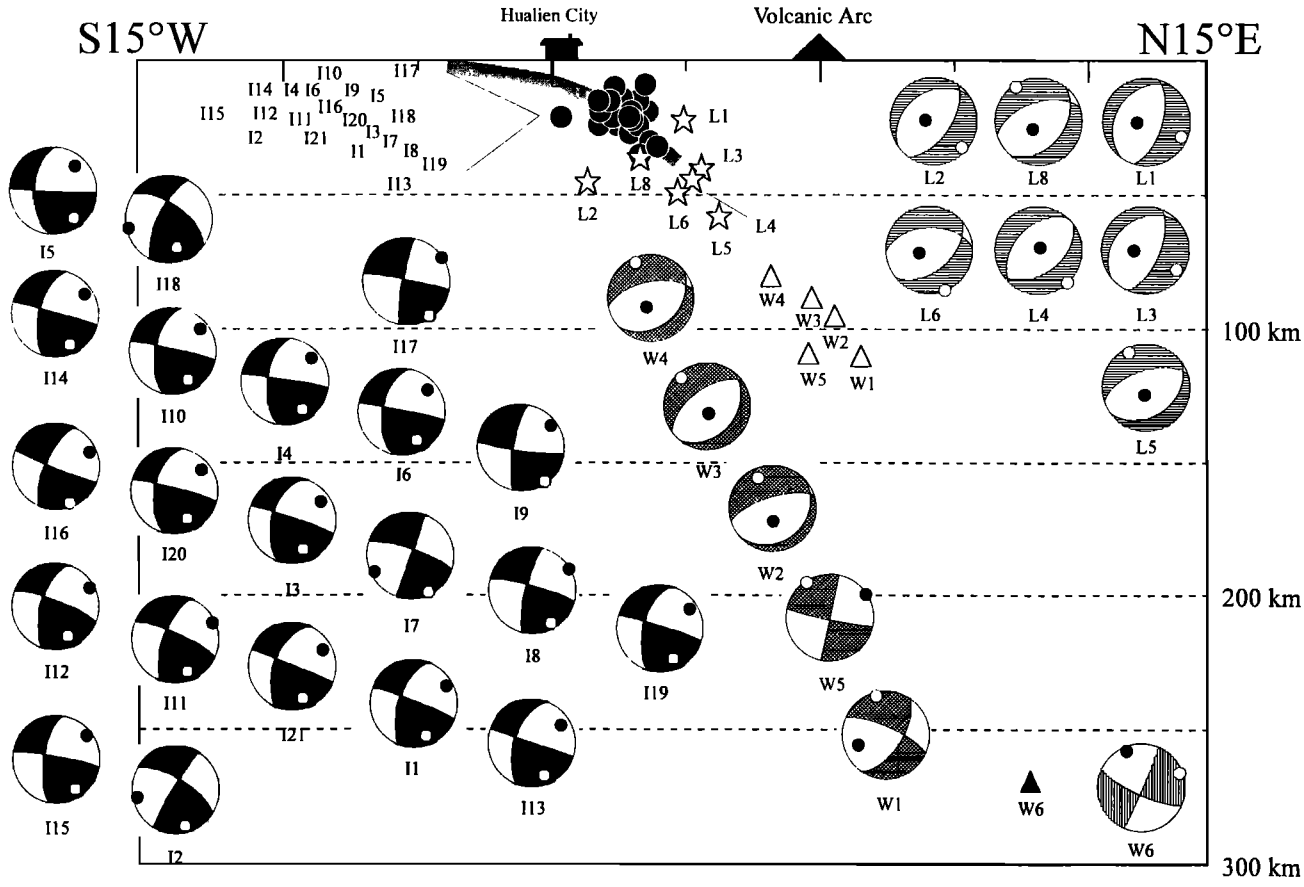

Figure 4. N15°E–S15°W cross section (without vertical exaggeration) of the southernmost Ryukyu arc. Hypocenters (small symbols) and focal mechanisms (large spheres) of earthquakes provide an outline of the configuration of the subducted Philippine Sea plate. Fault plane solutions are shown in equal-area projections of the back hemispheres of the focal sphere. Symbols are the same as in Figure 2a. Dashed lines mark depths at 50 km intervals. Earthquakes associated with low-angle thrust faulting, presumably representing the location of plate interface (thick shaded curve), occurred over limited depths between 10 and 35 km. The inferred subducted plate is in downdip extension between 80 and 120 km (events W1–5) but in downdip compression at ~270 km (event W6). A group of earthquakes showing lateral compression is found between the interface events and the Wadati-Benioff zone, probably due to the collision-related lateral compression.

slab beneath the southernmost Ryukyu arc (7 x cos70° x sin65°) given that the convergence obliquity, slab dip, and convergent rate are 70°, 65°, and 7 cm yr^{-1}, respectively [e.g., *Seno et al.*, 1993]. In contrast, the vertical descending rate is more than 2.5 times larger at the neighboring southern Ryukyu slab (~5.2 cm yr^{-1}) where the convergence obliquity is only 20° [*Liu et al*, 1995], even though the convergent rate (6.8 cm yr^{-1}) is slightly slower.

2.4. Lateral Compression Seismic Zone (LCSZ; Events L1–L10)

As shown in Figure 2, events L1–L10 between ISZ and WBSZ show thrust or oblique-thrust faulting. Their epicenters are distributed to the north of CSZ in the direction N70±10°W ending at the northern extension of CSZ.

These events have consistent orientation of *P* axes in the direction of the structure's strike (Figures 2 and 4), a pattern similar to that found in the southern and part of northern Ryukyu arcs [*Kao and Chen*, 1991]. They are at the same depths as events in CSZ (~10–60 km). However, most of them occurred between 40 and 60 km, as compared to less than 20 km for the CSZ. This feature is similar to the laterally compressional events observed beneath the Ryukyu arc [*Kao and Chen*, 1991], a subject discussed in section 3.

Note that 8 (L1–L6, L8, and L10) out of the 10 such events have *T* axes in the downdip direction and most of them occurred to the east of 122.1°E, directly downdip of the ISZ and and updip of WBSZ. Their focal mechanisms resemble some downdip extensional events (e.g., W2–W4) in WBSZ, suggesting possible influence of the stress field in WBSZ.

2.5. Okinawa Seismic Zone and Other Normal-Faulting Earthquakes (OSZ; Events O1–O6)

We find six events showing normal-faulting mechanisms (O1–O6, Figure 2). Event O6 took place within the Okinawa trough, a region of backarc extension in the Ryukyu subduction system [e.g., *Herman et al.*, 1978; *Shiono et al.*, 1980; *Eguchi and Uyeda*, 1983; *Kimura*, 1985; *Sibuet et al.*, 1987; *Kao and Chen*, 1991], whereas events O1 and O2 took place in northeast Taiwan. Since there is increasing evidence that northeast Taiwan is affected by the extensional process of Okinawa trough [e.g., *Yeh et al.*, 1989; *Liu*, 1995], we discuss

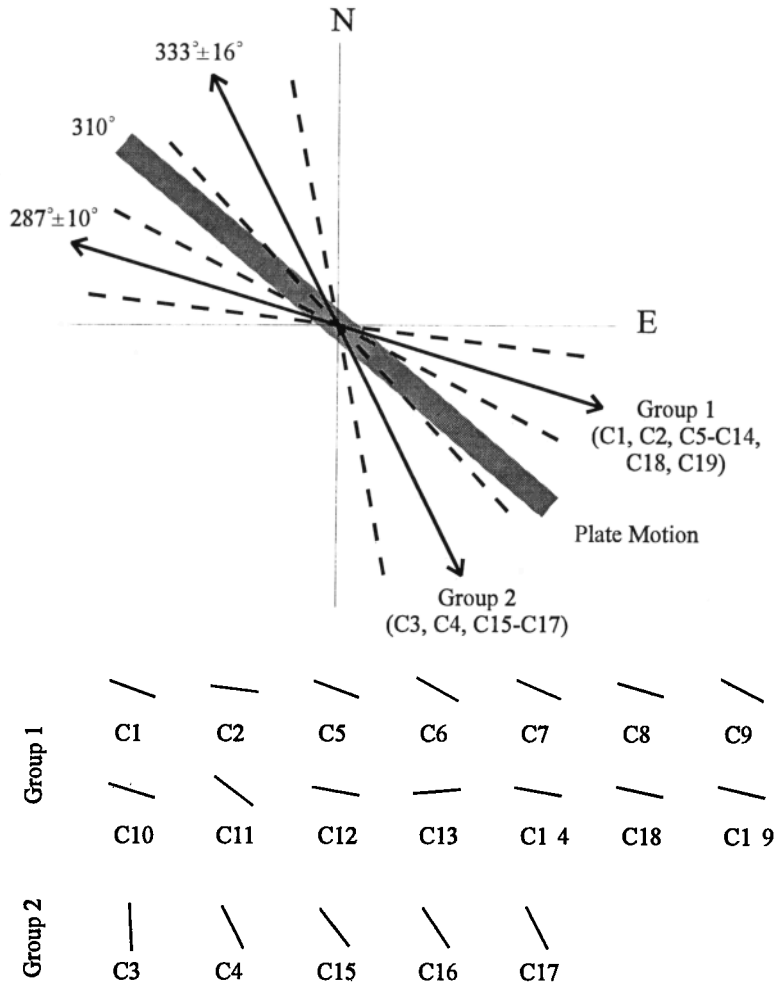

Figure 5a. Strain partition associated with earthquakes in the CSZ. The orientations of individual *P* axes are shown at bottom. They can be divided into two groups with average directions along 287° and 333°, respectively. The dashed lines represent the boundary of one standard deviation, whereas the thick shaded line indicates the direction of relative plate motion between the Philippine Sea and Eurasia plates [*Seno et al.*, 1993].

these three events as a group and call the corresponding structure "Okinawa Seismic Zone" (OSZ).

In Figure 3, the OSZ is characterized by shallow earthquakes occurred between ~24.6°N and 25°N. An interesting feature seems to be a systematic rotation of maximum tension axes from N–S for event O6, which agrees with the inferred extensional direction of the Okinawa trough [e.g., *Herman et al.*, 1978; *Kimura*, 1985; *Sibuet et al.*, 1987; *Sato et al.*, 1994], to NW–SE and nearly E–W for events O2 and O1, respectively (Figure 2a). This pattern may reflect the gradual changing state of strain associated with the crustal deformation of the Okinawa opening.

Two normal-faulting events (O3 and O5) were located to the south of ISZ. Event O3 has *T* axis in approximately N–S direction, perpendicular to the southernmost Ryukyu trench and thus may be due to bending of the subducted Philippine Sea plate. Event O5 has two subevents at depths of 35 and 10 km. The second (shallower) subevent shows typical normal faulting, whereas the first shows a horizontal or vertical dip-slip focal mechanism. One possible scenario is that event O5 is a listric normal fault which initiated along a horizontal plane at depth, then propagates upward with increasing dip, or, alternatively, they are actually two separated events such that the deeper one triggers the occurrence of the shallow.

Event O4 is in the Central Range just to the west of CSZ and Longitudinal Valley and is very shallow (5 km deep) with *T* axis parallel to the overall structural trend of Taiwan. Similar shallow normal-faulting events of smaller magnitudes were reported by *Rau* [1996], using data from the local network.

3. Tectonic Implications and Discussion

Subduction and collision are two completely different processes with significant variation in the distribution and characteristics of seismogenic structures. In subduction zones, the predominant seismogenic structure is the interplate thrust zone along which the oceanic lithosphere underthrusts the overriding plate [*Isacks et al.*, 1968]. Other major features include the Wadati-Benioff zone, earthquakes in the outer rise region, and sometimes intraplate events in the vicinity of plate interface or in the backarc. Collision zones, on the other hand, are characterized by active orogeny that leads to intense deformation in the lithosphere and complex

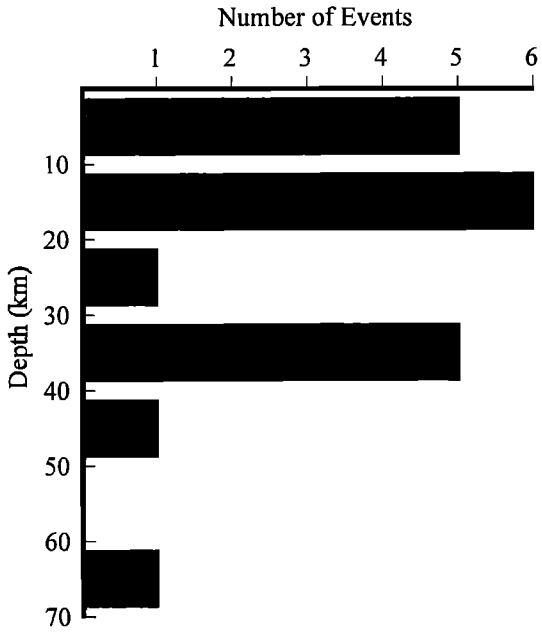

Figure 5b. Depths of the CSZ earthquakes show bimodal distribution with peaks at ≤20 km and 30–40 km.

mountain-and-range topography [e.g., *Molnar and Tapponnier*, 1975, 1978; *Molnar and Chen*, 1982; *Avouac and Tapponnier*, 1993; *Matte et al.*, 1996]. Regions adjacent to collision zones, meanwhile, would rotate significantly in response to the indentation [e.g., *Tapponnier et al*, 1982; *Armijo et al.*, 1986; *Burchfiel et al.*, 1989; *Chen et al.*, 1993; *Lue et al.*, 1995].

In the southernmost Ryukyu–Taiwan region, the rapid transition from oblique subduction to collision is most intriguing because it involves all major seismogenic structures and is accomplished within a very short distance (<150 km). In this section, we discuss how such transition is accomplished on the basis of our observations

3.1. Collision, Lateral Compression, and Orogenic Processes

We interpret both the CSZ and the LCSZ in terms of collision between the Philippine Sea and Eurasia plates, based on the consistent orientation of *P* axes with respect to the direction of relative plate convergence (Figures 2, 4, and 5). Under the overall tectonic framework of the region, this is probably also the most straightforward explanation [e.g., *Biq*, 1972; *Bowin et al*, 1978; *Wu*, 1978; *Tsai*, 1986].

Kao and Chen [1991] reported five earthquakes showing compression parallel or subparallel to the local strike of the Ryukyu arc and inferred that these events were resulted from the compressive strain transmitted through the subducted plate due to the collision between the western edge of the Ryukyu slab and the Eurasia plate near Taiwan. Our discovery of LCSZ supports such an inference. Our observation also indicates that the number of laterally compressional events is several times more than that found along the southern Ryukyu arc, suggesting that the compressive strain must originate from the collision zone and gradually fades out as it is transmitted across the subducted Ryukyu slab.

To further characterize the seismic deformation associated with the collision, we calculate the corresponding strain tensor by summing seismic moment tensors of all CSZ earthquakes (Appendix B). The corresponding eigenvalues are -3.56×10^{-6} (compression), 1.14×10^{-7}, and 3.44×10^{-6} (extension) with their corresponding eigenvectors along (-0.91, 0.40, 0.11), (-0.39, 0.92, 0.07), and (0.13, 0.02, 0.99), respectively. In terms of azimuth and plunge, they are (113, 6), (157, 0), and (261, 82), indicating that the predominant deformation is the horizontal shortening and a comparable extension in the vertical direction. Averaging over the observation window from 1964 to 1995, the maximum compressive strain rate is 1.2×10^{7} yr^{-1} along 293° (N67°W). Note that these results are subjected to an uncertainty of at least 50%, given the short time window of observation, uncertainties in source parameters, and different estimation of the seismogenic volume.

Our results may be compared with a recent study by *Pezzopane and Wesnousky* [1989], who use different events and seismogenic volumes. Taking the Taiwan region as a whole, *Pezzopane and Wesnousky* [1989] reported a maximum compressive axis in almost E–W direction, deviating more than 20° from ours. However, their calculated strain rate and direction became remarkably consistent with ours if only the largest events scattered throughout southeast Taiwan and offshore are taken into account. Furthermore, the present-day stress pattern from shallow microearthquakes in the Coastal Range reveals the same direction of maximum compression as ours [*Barrier and Angelier*, 1986]. The agreement among different observations presumably implies a uniform strain field throughout southeastern Taiwan region.

The above mentioned uniformity may have existed for a long time, as shown by the paleostress study in the Coastal Range [*Barrier and Angelier*, 1986]. The Coastal Range is made of a volcanic basement (the Chimei Igneous Complex and the Tuluanshan Formation of andesitic origin) overlain by a thick terrigeneous sequence (the Takangkou Formation) and Lichi mélange [*Ho*, 1988]. Analysis of fault orientations revealed two main periods of brittle deformation: the earlier extensional tectonics found only in the Takangkou Formation followed by the more recent compressional tectonics recorded

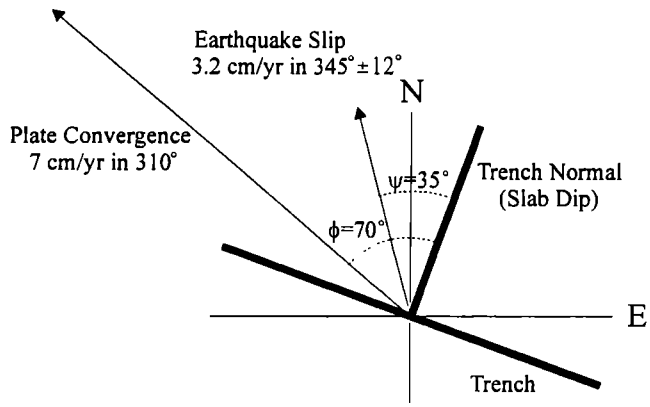

Figure 6. Slip partition associated with the ISZ earthquakes. The trench normal direction is inferred from the dip of subducted lithosphere. The average earthquake slip direction is in between the inferred trench normal and plate convergence directions. Seismic slip along the interface is estimated to be 3.2 cm yr^{-1} from accumulated seismic moments.

in all Coastal Range formations [*Barrier and Angelier*, 1986]. The direction of compression was inferred to be ~300° and has remained roughly constant since the orogeny began ~2 Ma. This result is also confirmed by a recent analysis of fault slip data and mechanical twin sets in calcite found in the Coastal Range [*Lin*, 1997].

It should be noted that our (as did *Pezzopane and Wesnousky* [1989]) derivation of strain tensor completely ignores the contribution from smaller ($m_b \leq 5.4$) earthquakes. On the basis of local data and the well-known moment–magnitude relation [*Hanks and Kanamori*, 1979] and the frequency–magnitude relation [*Gutenberg and Richter*, 1944], the total seismic moment released by earthquakes with $3.0 \leq m_b \leq 5.4$ in the entire Taiwan region over the observation time window is ~9.5 x 10^{18} N m, less than 3% of that calculated from CSZ earthquakes listed in Table 1. Thus, ignoring smaller earthquakes in our calculation seems well justified.

The observation that most CSZ events occurred to the east of the Longitudinal Valley may suggest that the geological material there (Coastal Range) is weaker than that to the west of the Longitudinal Valley (i.e., the Central Range). This suggestion, however, contradicts conventional thinking of Taiwan arc-continent collision in which a strong oceanic backstop (the Luzon arc) is indenting the weaker southeast Asia continent [e.g., *Suppe*, 1980, 1981]. Alternatively, our observation may imply that the Central Range, particularly its middle and lower crust, has a much lower effective strength such that it cannot accumulate seismogenic strain needed to generate earthquakes. Some recent studies seem to favor such an interpretation, arguing that the extremely low strength is either due to the high-temperature gradient [e.g., *Barr and Dahlen*, 1989; *Hwang and Wang*, 1993; *Wang et al.*, 1994; *Wu et al.*, 1997] or different rheology/composition [e.g., *Barr and Dahlen*, 1989; *Song et al.*, 1997].

The bimodal distribution of focal depths in CSZ (Figure 5b) may reflect the rheological variation in the lithosphere, as reported by *Chen and Molnar* [1983] for several regions of recent continental convergence. Combining experimental results from rock mechanics, they interpreted that the top and bottom layers of seismicity occur in the upper crust and uppermost mantle, respectively, with the lower crust being essentially aseismic. Adapting such an argument, we infer the Moho depth associated with CSZ to be between 25 and 35 km, in agreement with a tomographic image study that covers part of the northern portion of CSZ [*Rau and Wu*, 1995]. This conclusion can be easily tested should large-scale offshore deep reflection and/or ocean bottom seismometer (OBS) experiments be conducted in the region.

3.2. Oblique Subduction, Deformation in the Okinawa Trough, and Interplate Coupling

As shown in Figure 6, the convergence obliquity (ϕ) in the southernmost Ryukyu arc–Taiwan region is as large as 70±10°. The slip vectors associated with earthquakes showing low-angle thrust faulting (events I1–I21) have an average direction of 345° with a standard deviation of 12°. Hence the so-called earthquake slip obliquity (ψ) and the slip vector residual (ϕ - ψ, *McCaffrey* [1992]) are both ~35°.

McCaffrey [1992, 1994, 1996] reported that for regions with small ϕ, there often is no slip partitioning, whereas for regions with large ϕ, the degree of partition seems to vary significantly. The occurrence of great (M>8.0) subduction earthquakes often correlates with little slip partition. He proposed a model based on the rheological behavior of the forearc to interpret the observed correlation. Specifically, if the deformation in the forearc is more elastic such that both the lateral and trench-normal components of the relative plate motion can be stored as elastic strain, then interplate thrust events result in a slip direction close to the relative plate convergence and a larger magnitude. On the other hand, if the shear strength of the forearc is relatively small such that permanent shear deformation in the forearc takes place due to lateral component of the relative plate motion, then the occurrence of interface events could reflect only the trench-normal elastic strain, thus showing slip partitioning. In such a case, structures reflecting shear deformation in the overriding plate are expected, such as large strike-slip faults.

In the southernmost Ryukyu region, three large right-lateral strike-slip fault systems extending from the Ryukyu forearc across the Okinawa backarc basin were identified from detailed bathymetry as well as gravity and magnetic anomaly data [*Hsu et al.*, 1996]. Seismic reflection profiles also indicate very thick sediments in the forearc basins and a narrower accretionary prism to the west of 122.3°E [*Lallemand et al.*, 1997]. Furthermore, numerous bathymetric features resemble strike-slip faults were mapped out by a recent bathymetric survey in the region (C.-S. Liu, personal communication, 1997). Thus a significant amount of shear deformation exists in the overriding plate, and the plate interface in this region is unlikely to generate great (M>8.0) interplate thrust earthquakes.

Indeed, the sum of seismic moment release by the ISZ earthquakes is 3.74 x 10^{19} N m. If we assume the corresponding fault area to be 47 km long by 28 km wide (Figures 2 and 4), then the seismic slip is ~95 cm, and the average seismic slip rate is ~3.2 cm yr^{-1}. To close the vector circuit would require a slip rate of ~4.7 cm yr^{-1} in the direction of 288°, possibly by deformation in the forearc and aseismic slip along the plate interface.

In a global study, *Liu et al.* [1995] reported an average value of 0.5±0.2 for ψ/ϕ ratios for most oblique subduction zones. Although *Liu et al.* [1995] decided to exclude the Ryukyu arc from their analysis because of the data's internal inconsistency, we find that at least for the southernmost portion of the Ryukyu arc, their assessment is remarkably consistent with our observation.

In our study area, the seismogenic portion of the plate interface spans from a depth at 10 km (event I10, Figure 4) to 35 km (event I13). This is different from the rest of the Ryukyu–Kyushu arc where the interplate thrust zone is aseismic down to ~25–30 km but seismogenic between ~30 and ~50 km [*Kao and Chen*, 1991]. *Kao and Chen* [1991] studied the thermomechanical properties of the Ryukyu interface from heat flux measurements and reported a very low coefficient of friction of 0.10±0.05. They concluded that the appearance of low-angle thrust earthquakes at ~25–30 km implies that the plate interface has reached seismogenic strength there and that the termination of interface seismogenesis at ~50 km is due to increasing temperature (thus decreasing strength) at depth. We speculate that their concluded thermomechanical properties might be applicable to the southernmost Ryukyu arc between 10 and 35 km. Unfortunately, we are unable to verify this conclusion due to the lack of reliable heat flux measurements.

3.3. Configuration of the Present-Day Plate Boundary

The location and geometry of plate boundary in the Taiwan region have long been a controversial issue. On the basis of the "thin-skinned" critical taper model, *Bowin et al.* [1978] and *Suppe* [1980, 1981] proposed the deformation front between the Western Foothills and the Coastal Plain in west Taiwan to be the surface projection of the plate boundary between the Philippine Sea plate and Eurasia plate (Figure 2b). *Lu and Hsü* [1992] studied the lithology of Taiwan and argued that the deformation front is an intraplate structure. They concluded the Lishan fault in the Central Range to be the plate boundary (Figure 2b). On the other hand, *Biq* [1971, 1972] placed the plate boundary along the Longitudinal Valley (Figure 2) based on the fact that the Western Foothills and Central Range are composed of rocks belonging to the passive margin of southeast Asia whereas strata in the Coastal Range are mainly associated with the former Luzon arc.

Our results can provide some insight to resolve this controversy. We interpreted the ISZ as the plate boundary between the Eurasia and Philippine Sea plates (Figures 2b and 4). The geometry of ISZ is such that it gradually bends northward with increasing dip angle as it approaches Taiwan. The ISZ becomes very steep where it meets the northern terminus of CSZ (Figure 2b). Our observations show no evidence that the ISZ is directly connected to the deformation front in west Taiwan or the Lishan fault, as previous studies suggested. Therefore we conclude that the present-day plate boundary between the Philippine Sea and Eurasia plates in the study area is represented by the ISZ and the Longitudinal Valley.

Our inference of the plate boundary is supported by a recent study of crustal velocity structures in the area. Using seismic refraction data from both onshore and offshore experiments, *Cheng et al.* [1996] concluded that the seismic velocity signature of the Coastal Range can be traced north to 24.2°N, then the velocity anomaly bends clockwise sharply by ~120–130° and extends into the offshore. This pattern is consistent with the geometry inferred from the shallow portion of the ISZ and CSZ (Figure 2b). On the other hand, the seismic velocity signature of the Central Range extends farther north and can be correlated with that of the (overriding) Ryukyu arc, suggesting that the Central Range and the islands of Ryukyu arc probably share the same tectonic origin.

3.4. Strain Patterns in the Subducted Slab

The Ryukyu–Kyushu arc is known for strain segmentation in the subducted Philippine Sea plate [*Shiono et al.*, 1980; *Kao and Chen*, 1991]: while intermediate-depth earthquakes in the northern Ryukyu arc consistently show downdip extension to a depth of 200 km, those in southern Ryukyu show downdip compression to a depth of 270 km near Taiwan [*Kao and Chen*, 1991; *Shiono et al.*, 1980]. In the present study, we found downdip extension at depths between 80 and 120 km (events W1–W5, Figures 2 and 4) and downdip compression at 270 km (event W6) with transition between 120 and 260 km.

On a global scale, *Fujita and Kanamori* [1981] showed that old and slow slabs are mostly dominated by downdip extensional events, while young and slow or old and fast slabs are either in downdip compression or show a mixture of both. Combining their arguments and data from the Ryukyu–Kyushu arc, *Kao and Chen* [1991] concluded that within a given segment, extensional strain can be correlated with either an older age of the downgoing slab or a slower rate of convergence.

The change of strain patterns within the subducted Ryukyu slab occurs in a very narrow zone between 123 and 124°E (compare Figure 2a and Figure 2 of *Kao and Chen* [1991]) and seems to correlate with a sharp change in the directions of horizontal displacements, as determined by Global Positioning System (GPS) measurements [*Imanishi et al.*, 1996]. Incidentally, it occurs at exactly the place where the Gagua Ridge intercepts the Ryukyu trench such that the convergence obliquity has a sharp variation (Figure 1). The subduction of Gagua Ridge beneath the Ryukyu arc, though largely unknown, seems to have significantly affected the development of regional tectonic structures [e.g., *Hsu et al.*, 1996]. From the distribution of magnetic anomalies [*Hilde and Lee*, 1984], it is inferred that the ocean floor being subducted along the southernmost Ryukyu arc to the west of the Gagua Ridge is only slightly younger (~1–2 Ma) than that to the east (chrons 16 and 17, Figure 1). However, owing to the large convergence obliquity (~70°, Figure 6), the downgoing slab beneath the southernmost Ryukyu arc is descending at a rate of ~2.2 cm yr^{-1}, less than a half of the ~5.2 cm yr^{-1} rate in the southern Ryukyu arc [*Seno et al.*, 1993]. Thus the subducted slab in the studied region is subjected to a relatively large negative buoyancy force (slab pull) that results in downdip extension at intermediate depth. The existence of a downdip compressional earthquake at ~270 km implies that the downgoing slab probably encounters strong resistance at that depth. Unfortunately, no data are available to provide constraint on the transition between depths of 120 and 260 km.

3.5. Normal-Faulting Earthquakes

As we have described in section 2.5, normal-faulting earthquakes in the region can be roughly divided into three groups, namely, the OSZ, those events in the outer rise, and an earthquake in the Central Range.

Interaction between the opening of Okinawa trough and collision along east Taiwan has been recognized as playing a crucial role in determining the regional stress patterns [e.g., *Cheng*, 1995; *Hu et al.*, 1996]. Using a two-dimensional (2-D) numerical model with elastic and elasto-plastic rheologies, *Hu et al.* [1996] showed that the maximum tension in the Okinawa trough rotates significantly from approximately N–S to approximately NW–SE with rapidly decreasing magnitude as it approaches northeast Taiwan. Similarly, the trajectory of the maximum compression follows the relative convergence direction along the Longitudinal Valley but gradually turns to approximately NE–SW and nearly diminishes in northeast Taiwan. The transition zone between these two stress regimes coincides with the place where OSZ, ISZ, CSZ, and LCSZ all meet together (Figure 2b). The observation of successive rotation of T axes among events O6, O2, and O1 confirms the numerical simulation result and may imply that the northeast Taiwan region is currently under the influence of both the extension from Okinawa trough opening and the compression from the collision between the Philippine Sea and Eurasia plates.

We interpret events 3 and 5 as reflecting the extension due to the bending of the subducted Philippine Sea plate [e.g., *Forsyth*, 1982]. *Christensen and Ruff* [1983, 1988] suggested that for a strongly coupled subduction zone, outer rise events would show alternative patterns of compression and extension before and immediately after, respectively, a large interface earthquake. Since outer rise compressional earthquakes are nowhere found along the entire Ryukyu–Kyushu arc [*Kao and Chen*, 1991] and that the region appears to be devoid of major shallow earthquakes [e.g., *Abe*, 1981; *Kanamori*, 1986], we conclude that the plate interface is probably not strongly coupled. This is, again, consistent with our previous conclusions.

Finally, we discuss the significance of event O4, in the Central Range just to the west of the Longitudinal Valley, which has a very shallow depth (5 km, Figure 2a) and a T axis approximately perpendicular to the direction of maximum compression. Such occurrence may be interpreted as a consequence of the delamination in the upper mantle that leads to rapid rising of mantle materials to shallow depths [e.g., *England and Houseman*, 1989; *England and Molnar*, 1993]. Perhaps like Tibet, the nature of the orogeny in Taiwan has changed from "thin-skinned" deformation [e.g., *Chapple*, 1978; *Suppe*, 1981; *Davis et al.*, 1983] to lithospheric collision involving the whole crust and uppermost mantle [e.g., *Hwang and Wang*, 1993; *Wang et al.*, 1996; *Wu et al.*, 1997].

4. Summary and Conclusion

By detailed analysis of seismicity and source parameters of 62 large and moderate-sized earthquakes ($m_b \geq 5.5$) that occurred in the southernmost Ryukyu–Taiwan region, we investigate the characteristics of transition from a typical oblique subduction zone to an active collision zone. On the basis of our results, five major seismogenic structures were delineated. They are the Collision Seismic Zone (CSZ), the Interface Seismic Zone (ISZ), the Wadati-Benioff Seismic Zone (WBSZ), the Lateral Compression Seismic Zone (LCSZ), and the Okinawa Seismic Zone (OSZ).

The CSZ, located along the east coast of Taiwan and offshore (Figure 2), is the predominant seismogenic structure in the region. Most CSZ events show thrust or strike-slip faulting with their P axes distributing in two groups: one along 287°±10° and another 333°±16° (Figure 5a). Since the predicted relative plate motion (310°) is in between these two directions, we interpret such a pattern as a result of strain partition in the region. Furthermore, earthquakes showing approximately E–W compression are about twice as many as those showing N–S or NW–SE compression. The majority of CSZ earthquakes occur at shallow depth (≤20 km) and between 30 and 40 km.

The seismic strain tensor derived from the summation of seismic moment tensors of CSZ events indicates that the associated seismic deformation is a combination of roughly equal amounts of horizontal shortening and vertical extension, perhaps due to collision and orogeny, respectively. The maximum compressive strain rate is 1.2×10^{-7} yr^{-1} along 293°. This result is consistent with that estimated from the largest events scattered in southeast Taiwan and offshore and the paleostress distribution in the Coastal Range for the past ~2 Myr. Thus we conclude that the compressive strain field resulted from the collision is quite uniform throughout the southeast Taiwan region.

The geometry of the ISZ is distorted significantly toward its westernmost end (Figure 2b). It can be approximated by a north dipping plane that is pushed northward with increasing dip as it approaches Taiwan. The seismogenic portion of the interface has a depth range from ~10 to ~35 km, much shallower than observed elsewhere along the Ryukyu arc. The slip vector residual is as large as 35°, implying a low probability for the occurrence of great (M>8) subduction earthquakes. This conclusion is consistent with the speculation that the plate interface has a very low coefficient of friction based on similar thermomechanical properties estimated for the rest of Ryukyu arc.

Seismic strain patterns within the subducted Philippine Sea slab show predominantly downdip extension for depths between 80 and 120 km but downdip compression at ~270 km (Figures 2 and 4). This change in patterns is different from what has been observed along the rest of the Ryukyu arc, where only a single seismic pattern is associated with a given segment of the arc (i.e., strain segmentation [*Kao and Chen*, 1991]). We interpret the change of strain patterns in the Wadati-Benioff zone as a combined result of both oblique subduction and the slab's negative buoyancy.

Earthquakes in the LCSZ show a mixture of thrust and oblique strike-slip with P axes in approximately E–W direction, roughly parallel to the local strike of the trench-arc system. Hypocenters of these events are distributed between ISZ and WBSZ along a structure striking 110±10°. We interpret these events to be caused by compressive strain due to the collision between the Philippine Sea and Eurasia plates in east Taiwan. Such a structure extends throughout southern and part of northern Ryukyu arcs, as evidenced by similar but fewer events there.

Shallow normal-faulting events in the region occur in three different structures: the backarc region presumably reflecting the extension associated with the opening process of the Okinawa trough; the outer rise probably due to the bending of the Philippine Sea plate; and the Central Range to the west of CSZ. The transition from extension in the Okinawa trough to compression in the collision zone is characterized by a successive rotation of earthquake T axes from approximately N–S to approximately E–W. The normal event in the Central Range has its maximum extension roughly parallel to the structural trend of Taiwan. This pattern mimics what is observed in high Tibet and may imply that the orogeny in Taiwan has changed from "thin-skinned" deformation to lithospheric collision involving the whole crust and uppermost mantle.

Appendix A

We present the result of joint hypocenter determination (JHD [*Dewey*, 1972]) for selected events in Table 1. We fixed the focal depths at the ones determined by our waveform inversion. The relocated epicenters are listed and plotted in Table A1 and Figure A1, respectively, along with that reported by the International Seismological Centre (ISC) or Preliminary Determination of Epicenters (PDE) and by the local network.

In the most general terms, the JHD results do not indicate that possible mislocation could result in any radical change of

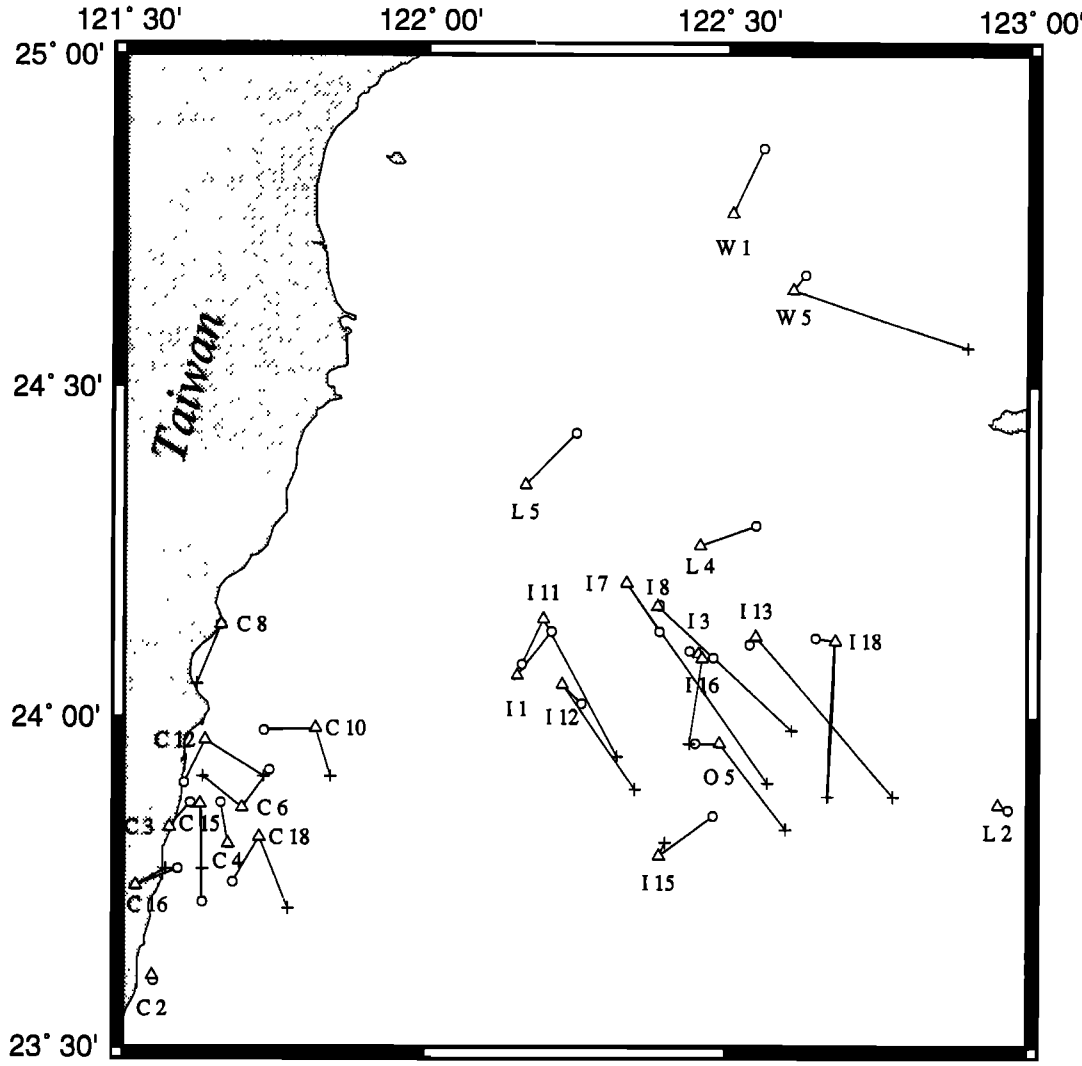

Figure A1. Map showing the results of JHD. Epicenters determined by JHD (triangles) are plotted along with that reported by the ISC or PDE (circles) and by the local network (crosses). Event numbers are according to Table 1 and marked besides the JHD locations.

our interpretations. In fact, for most cases, the differences between ISC or PDE and our JHD locations are less than 0.1°. When compared to the epicenters reported by the local network, however, the discrepancy varies depending on whether or not the earthquakes occurred inside the local network. For a few events belonging to ISZ or WBSZ, the differences can be as large as 0.4° (e.g., events I7 and W5, Figure A1), probably due to a combined effect from the uneven distribution of local stations as well as the fact that all these events occurred outside the network. Similar conclusion is reached by a controlled study using synthetic data [*Tsai and Wu*, 1996].

Appendix B

We show the detail of calculating the seismic strain tensor associated with earthquakes in CSZ. The method is based on the work by *Kostrov* [1974], who derived the seismic strain tensor (ε_{ij}) by summing moment tensors (M_{ij}) of individual earthquakes,

$$\varepsilon_{ij} = \frac{1}{2\mu V}\left(\sum_{x=1}^{n} M_{ij}^{(x)}\right) \tag{B1}$$

where μ and V are the rigidity (assumed to be 3×10^{11} dyn cm^{-2}) and seismogenic volume, respectively. The sum of moment tensors (x 10^{17} N m) for events C1–C19 is

-1292	605	356
605	-213	-49
356	-49	1505

where the convention is that extension is positive and the 1, 2, 3 axes point east, north, and vertically up, respectively. If we assume the dimension of the seismogenic volume of the CSZ to be 150 km long by 100 km wide by 50 km thick, as estimated from Figures 1–4, then the corresponding seismic strain tensor (x10^{-7}) is

-28.7	13.4	7.9
13.4	-4.7	-1.1
7.9	-1.1	33.4

Table A1. Results of JHD Relocation for Selected Earthquakes

Event[a]	ISC/PDE Lat., Long.	Local Network Lat., Long.	JHD Lat., Long.
C2	23.60, 121.55	-	23.608, 121.548
C3	23.87, 121.61	-	23.833, 121.576
C4	23.87, 121.66	-	23.808, 121.672
C6	23.92, 121.74	23.91, 121.63	23.862, 121.695
C8	24.14, 121.66	24.05, 121.62	24.140, 121.660
C10	23.98, 121.73	23.91, 121.84	23.983, 121.815
C12	23.90, 121.60	23.91, 121.73	23.965, 121.634
C15	23.72, 121.63	23.77, 121.63	23.868, 121.626
C16	23.77, 121.59	23.77, 121.57	23.745, 121.520
C18	23.75, 121.68	23.71, 121.77	23.818, 121.723
I1	24.13, 122.21	-	24.063, 122.152
I3	24.10, 122.44	-	24.096, 122.455
I7	24.13, 122.39	23.90, 122.57	24.203, 122.335
I8	24.17, 122.39	23.98, 122.61	24.168, 122.387
I11	24.08, 122.16	23.94, 122.32	24.149, 122.196
I12	24.02, 122.26	23.89, 122.35	24.049, 122.228
I13	24.11, 122.54	23.88, 122.78	24.122, 122.550
I15	23.85, 122.48	23.81, 122.40	23.790, 122.390
I16	24.09, 122.48	23.96, 122.44	24.089, 122.461
I18	24.12, 122.65	23.88, 122.67	24.116, 122.683
L2	23.86, 122.97	-	23.867, 122.953
L4	24.29, 122.55	-	24.260, 122.457
L5	24.43, 122.25	-	24.352, 122.165
W1	24.86, 122.56	-	24.762, 122.509
W5	24.67, 122.63	24.56, 122.90	24.647, 122.610
O5	23.96, 122.45	23.83, 122.60	23.960, 122.490

[a]Event number according to Table 1.

The eigenvalues are -3.56×10^{-6}, 1.14×10^{-7}, and 3.44×10^{-6} with their corresponding eigenvectors along (-0.91, 0.40, 0.11), (-0.39, 0.92, 0.07), and (0.13, 0.02, 0.99), respectively. In terms of azimuth and plunge, they are (113, 6), (157, 0), and (261, 82). Averaging over the observation window from 1964 to 1995, the corresponding strain rates are -1.2×10^{-7}, 3.8×10^{-8}, and 1.1×10^{-7} yr^{-1}.

Acknowledgments. We thank John Nábelek for a copy of his waveform analysis code. We also benefited from discussion with Wang-Ping Chen, Ling-Yun Chiao, Shu-Kun Hsu, Jyr-Ching Hu, Ban-Yuan Kuo, Jian-Cheng Lee, Wen-Tsung Liang, Char-Shine Liu, Lin-Gun Liu, Chia-Yu Lu, Ruey-Juin Rau, Chi-Yuen Wang, and Francis T. Wu. Thoughtful reviews by Chi-Yu King (the Associate Editor), Rob McCaffrey, and Ta-Liang Leon Teng significantly improved the manuscript. Mary Ann Glennon provided graphic programs for plotting our inversion results. Some figures are generated by the GMT software written by Paul Wessel and Walter H. F. Smith. Seismograms were collected from the IRIS DMS, the NEIC, and the Lamont-Doherty Earth Observatory. This research was partially supported by the National Science Council of Taiwan (grant NSC85-2111-M-001-020-Y) and the Central Weather Bureau (grant CWB84-2E-22).

References

Abe, K., Magnitudes of large shallow earthquakes from 1904 to 1980, *Phys. Earth Planet. Inter.*, *27*, 72–92, 1981.

Allen, C. R., Circum-Pacific faulting in the Philippine–Taiwan region, *J. Geophys. Res.*, *67*, 4795–4812, 1962.

Angelier, J., F. Bergerat, H.-T. Chu, and T.-Q. Lee, Tectonic analysis and the evolution of a curved collision belt: The Hsuehshan Range, northern Taiwan, *Tectonophysics*, *183*, 77–96, 1990.

Angelier, J., H.-T. Chu, and J.-C. Lee, Shear concentration in a collision zone: Kinematics of the Chihshang Fault as revealed by outcrop-scale quantification of active faulting, Longitudinal Valley, eastern Taiwan, *Tectonophysics, 274*, 117–143, 1997.

Armijo, R., P. Tapponnier, J. L. Mercier, and T.-L. Han, Quaternary extension in southern Tibet: Field observations and tectonic implications, *J. Geophys. Res.*, *91*, 13,803–13,872, 1986.

Avouac, J.-P., and P. Tapponnier, Kinematic model of active deformation in central Asia, *Geophys. Res. Lett*, *20*, 895–898, 1993.

Barr, T. D., and F. A. Dahlen, Steady-state mountain building, 2, Thermal structure and heat budget, *J. Geophys. Res.*, *94*, 3923–3947, 1989.

Barrier, E., and J. Angelier, Active collision in eastern Taiwan: The Coastal Range, *Mem. Geol. Soc. China*, *7*, 135–159, 1986.

Benioff, H., Seismic evidence for the fault origin of oceanic deeps, *Geol. Soc. Am. Bull.*, *60*, 1837–1856, 1949.

Benioff, H., Orogenesis and deep crustal structure: Additional evidence from seismology, *Geol. Soc. Am. Bull.*, *65*, 385–400, 1954.

Bevis, M., and B. L. Isacks, Hypocentral trend surface analysis: Probing the geometry of Benioff zones, *J. Geophys. Res.*, *89*, 6153–6170, 1984.

Biq, C.-C., Comparison of mélange tectonics in Taiwan and in some other mountain belts, *Petrol. Geol. Taiwan*, *9*, 79–106, 1971.

Biq, C.-C., Dual-trench structure in the Taiwan Luzon region, *Proc. Geol. Soc. China*, *15*, 66–75, 1972.

Bowin, C., R. S. Lu, C. S. Lee, and H. Schouton, Plate convergence and accretion in the Taiwan–Luzon region, *AAPG Bull.*, *62*, 1645–1672, 1978.

Burchfiel, B. C., Q. Deng, P. Molnar, L. Royden, Y. Wang, P. Zhang, and W. Zhang, Intracrustal detachment within zones of continental deformation, *Geology*, *17*, 748–752, 1989.

Chapple, W. M., Mechanics of thin-skinned fold-and-thrust belts, *Geol. Soc. Am. Bull.*, *89*, 1189–1198, 1978.

Chen, W.-P., and P. Molnar, Focal depths of intracontinental earthquakes and their implications for the thermal and mechanical properties of the lithosphere, *J. Geophys. Res.*, *88*, 4183–4214, 1983.

Chen, Y., V. Courtillot, J.-P. Cogné, J. Besse, Z. Yang, and R. Enkin, The configuration of Asia prior to the collision of India: Cretaceous paleomagnetic constraints, *J. Geophys. Res.*, *98*, 21,927–21,941, 1993.

Cheng, S.-N., The study of stress distribution in and around Taiwan, Ph.D. thesis, Natl. Cent. Univ., Chung Li, Taiwan, 1995.

Cheng, W.-B., C. Wang, and C.-T. Shyu, Crustal structure of the northeastern Taiwan area from seismic refraction data and its tectonic implications, *Terr. Atmos. Oceanic Sci.*, *7*, 467–487, 1996.

Christensen, D. H., and L. J. Ruff, Outer-rise earthquakes and seismic coupling, *Geophys. Res. Lett.*, *10*, 697–700, 1983.

Christensen, D. H., and L. J. Ruff, Seismic coupling and outer rise earthquakes, *J. Geophys. Res.*, *93*, 13,421–13,444, 1988.

Davis, D., J. Suppe, and F. A. Dahlen, Mechanics of fold-and-thrust belts and accretionary wedges, *J. Geophys. Res.*, *88*, 1153–1172, 1983.

DeMets, C., R. G. Gordon, D. F. Argus, and S. Stein, Current plate motions, *Geophys. J. Int.*, *101*, 425–478, 1990.

Dewey, J. W., Seismicity and tectonics of western Venezuela, *Bull. Seismol. Soc. Am.*, *62*, 1711–1751, 1972.

Dziewonski, A. M., T.-A. Chou, and J. H. Woodhouse, Determination of earthquake source parameters from waveform data for studies of global and regional seismicity, *J. Geophys. Res.*, *86*, 2825–2852, 1981.

Dziewonski, A. M., J. E. Franzen, and J. H. Woodhouse, Centroid-moment tensor solutions for April–June, 1983, *Phys Earth Planet. Inter.*, *33*, 243–249, 1983.

Dziewonski, A. M., J. E. Franzen, and J. H. Woodhouse, Centroid-moment tensor solutions for July–September, 1983, *Phys. Earth Planet. Inter.*, *34*, 1–8, 1984.

Dziewonski, A. M., J. E. Franzen, and J. H. Woodhouse, Centroid-moment tensor solutions for January–March, 1985, *Phys. Earth Planet. Inter.*, *40*, 249–258, 1985.

Dziewonski, A. M., G. Ekström, J. E. Franzen, and J. H. Woodhouse, Centroid-moment tensor solutions for January–March 1986, *Phys. Earth Planet. Inter.*, *45*, 1–10, 1987a.

Dziewonski, A. M., G. Ekström, J. E. Franzen, and J. H. Woodhouse, Global seismicity of 1977: Centroid-moment tensor solutions for 471 earthquakes, *Phys. Earth Planet. Inter.*, *45*, 11–36, 1987b.

Dziewonski, A. M., G. Ekström, J. E. Franzen, and J. H. Woodhouse, Global seismicity of 1978: Centroid-moment tensor solutions for 512 earthquakes, *Phys. Earth Planet Inter.*, *46*, 316–342, 1987c.

Dziewonski, A. M., G. Ekström, J. E. Franzen, and J. H. Woodhouse, Global seismicity of 1981: Centroid-moment tensor solutions for 542 earthquakes, *Phys. Earth Planet. Inter.*, *50*, 155–182, 1988.

Dziewonski, A. M., G. Ekström, J. H. Woodhouse, and G. Zwart, Centroid-moment tensor solutions for April–June, 1988, *Phys. Earth Planet. Inter.*, *54*, 199–209, 1989.

Dziewonski, A. M., G. Ekström, and M. P. Salganik, Centroid-moment tensor solutions for October–December, 1994, *Phys. Earth Planet. Inter.*, *91*, 187–201, 1995.

Dziewonski, A. M., G. Ekström, and M. P. Salganik, Centroid-moment tensor solutions for April–June, 1995, *Phys. Earth Planet. Inter.*, *96*, 1–13, 1996.

Eguchi, T., and S. Uyeda, Seismotectonics of the Okinawa Trough and Ryukyu Arc, *Mem. of Geol. Soc. China*, *5*, 189–210, 1983.

England, P., and G. Houseman, Extension during continental convergence, with application to the Tibetan Plateau, *J. Geophys. Res.*, *94*, 17,561–17,579, 1989.

England, P., and P. Molnar, Cause and effect among thrust and normal faulting, anatectic melting and exhumation in the Himalayas, *Spec. Publ. Geol. Soc. Am.*, *74*, 401–411, 1993.

Fan, G., J. F. Ni, and T. C. Wallace, Active tectonics of the Pamirs and Karakorum, *J. Geophys. Res.*, *99*, 7131–7160, 1994.

Fitch, T. J., Plate convergence, transcurrent faults, and internal deformation adjacent to southeast Asia and the western Pacific, *J. Geophys. Res.*, *77*, 4432–4460, 1972.

Forsyth, D. W., Determinations of focal depths of earthquakes associated with the bending of oceanic plates at trenches, *Phys. Earth Planet. Inter.*, *28*, 141–160, 1982.

Fujita, K., and H. Kanamori, Double seismic zones and stresses of intermediate depth earthquakes, *Geophys. J. R. Astron. Soc.*, *66*, 131–156, 1981.

Gutenberg, B., and C. F. Richter, Frequency of earthquakes in California, *Bull. Seismol. Soc Am.*, *34*, 185–188, 1944.

Hanks, T. C., and H. Kanamori, A moment magnitude scale, *J. Geophys. Res.*, *84*, 2348–2350, 1979.

Herman, B. M., R. N. Anderson, and M. Truchan, Extensional tectonics in the Okinawa trough, in *Geological and Geophysical Investigations of Continental Margins*, edited by J.S. Watkins, L. Montadert, and P.W. Dickinson, *Mem. Am. Assoc. Pet. Geol.*, *29*, 199–208, 1978.

Hilde, T. W. C., and C. S. Lee, Origin and evolution of the West Philippine Basin: A new interpretation, *Tectonophysics*, *102*, 85–104, 1984.

Ho, C. S., A synthesis of the geologic evolution of Taiwan, *Tectonophysics*, *125*, 1–16, 1986.

Ho, C. S., *An Introduction to the Geology of Taiwan*, 2nd ed., 192 pp., Cent. Geol. Surv., Minist. of Econ. Affairs, Taipei, 1988.

Hsu, S.-K., and J.-C. Sibuet, Is Taiwan the result of arc-continent or arc-arc collision?, *Earth Planet Sci Lett.*, *136*, 315–324, 1995.

Hsu, S.-K., J.-C. Sibuet, S. Monti, C.-T. Shyu, and C.-S. Liu, Transition between the Okinawa trough backarc extension and the Taiwan collision: new insights on the southernmost Ryukyu subduction zone, *Mar. Geophys. Res.*, *18*, 163–187, 1996.

Hu, J.-C., J. Angelier, J.-C. Lee, H.-T. Chu, and D. Byrne, Kinematics of convergence, deformation and stress distribution in the Taiwan collision area: 2-D finite-element numerical modeling, *Tectonophysics*, *255*, 243–268, 1996.

Hwang, W.-T., and C.-Y. Wang, Sequential thrusting model for mountain building: Constraints from geology and heat flow of Taiwan, *J. Geophys. Res.*, *98*, 9963–9973, 1993.

Imanishi, M., F. Kimata, N. Inamori, R. Miyajima, and K. Hirahara, Horizontal displacements by GPS measurements at the Okinawa–Sakishima Islands (in Japanese), *J. Seismol. Soc. Jpn.*, *49*, 417–421, 1996.

Isacks, B. L., and M. Barazangi, Geometry of Benioff zones: Lateral segmentation and downwards bending of the subducted lithosphere, in *Island Arcs, Deep Sea Trenches and Back-Arc Basins, Maurice Ewing Ser.*, vol. 1, edited by M. Talwani and W.C. Pitman III, pp. 99–114, AGU, Washington, D. C., 1977.

Isacks, B., J. Oliver, and L. R. Sykes, Seismology and the new global tectonics, *J. Geophys. Res.*, *73*, 5855–5899, 1968.

Jarrard, R. D., Relations among subduction parameters, *Rev. Geophys.*, *24*, 217–284, 1986a.

Jarrard, R. D., Terrane motion by strike-slip faulting of forearc slivers, *Geology*, *14*, 780–783, 1986b.

Kanamori, H., The Alaska earthquake of 1964: Radiation of long-period surface waves and source mechanism, *J. Geophys. Res.*, *75*, 5029–5040, 1970.

Kanamori, H., Rupture process of subduction-zone earthquakes, *Annu. Rev. Earth Planet. Sci.*, *14*, 293–322, 1986.

Kao, H., and W.-P. Chen, Earthquakes along the Ryukyu–Kyushu arc: Strain segmentation, lateral compression, and the thermomechanical state of the plate interface, *J. Geophys. Res.*, *96*, 21,443–21,485, 1991.

Kao, H., and W.-P. Chen, The double seismic zone in Kuril-Kamchatka: The tale of two overlapping single seismic zones, *J. Geophys. Res.*, *99*, 6913–6930, 1994.

Kao, H., and W.-P. Chen, Transition from interplate slip to double seismic zone along the Kuril–Kamchatka arc, *J. Geophys. Res.*, *100*, 9881–9903, 1995.

Kao, H., and W.-P. Chen, Seismicity in the outer-rise–forearc region and configuration of the subducting lithosphere with special reference to the Japan trench, *J. Geophys. Res.*, *101*, 27,811–27,831, 1996.

Kimura, M., Back-arc rifting in the Okinawa trough, *Mar. Pet. Geol.*, *2*, 222–240, 1985.

Kimura, M., S. Uyeda, Y. Kato, T. Tanaka, M. Yamano, T. Gamo, H. Sakai, S. Kato, E. Izawa, and T. Oomori, Active hydrothermal mounds in the Okinawa trough backarc basin, Japan, *Tectonophysics*, *145*, 319–324, 1988.

Kostrov, V. V., Seismic moment and energy of earthquakes, and seismic flow of rock, *Izv. Acad. Sci. USSR, Phys. Solid Earth*, *1*, 23–44, 1974.

Lallemand, S.E., C.-S. Liu, and Y. Font, A tear fault boundary between the Taiwan orogen and the Ryukyu subduction zone, *Tectonophysics*, *274*, 171–190, 1997.

Lee, T.-Y., and L. A. Lawver, Cenozoic plate reconstruction of the South China Sea region, *Tectonophysics*, *235*, 149–180, 1994.

Lin, C.-W., The deformation of the arc system in the Taiwan arc-continent collision, in *Proceedings of the 1997 Annual Meeting of the Geological Society of China*, pp. 359–363, Geol. Soc. of China, Tainan, 1997.

Liu, C.-C., The Ilan plain and the southwestward extending Okinawa trough, *J. Geol. Soc. China*, *38*, 229–242, 1995.

Liu, X., K. C. McNally, and Z.-K. Shen, Evidence for a role of the downgoing slab in earthquake slip partitioning at oblique subduction zones, *J. Geophys. Res.*, *100*, 15,351–15,372, 1995.

Lu, C.-Y., and K. J. Hsü, Tectonic evolution of the Taiwan mountain belt, *Petrol. Geol. Taiwan*, *27*, 21–46, 1992.

Lu, C.-Y., and J. Malavieille, Oblique convergence, indentation and rotation tectonics in the Taiwan Mountain Belt: Insights from experimental modelling, *Earth Planet. Sci. Lett.*, *121*, 477–494, 1994.

Lu, R. S., J. J. Pan, and T. C. Lee, Heat flow in the southwestern Okinawa trough, *Earth Planet. Sci. Lett.*, *55*, 299–310, 1981.

Lue, Y.-T., T.-Q. Lee, and Y. Wang, Paleomagnetic study on the collisional-related bending of the fold-thrust belt, northern Taiwan, *J. Geol. Soc. China*, *38*, 215–227, 1995.

Lukk, A. A., S. L. Yunga, V. I. Shevchenko, and M. W. Hamburger, Earthquake focal mechanisms, deformation state, and seismotectonics of the Pamir-Tien Shan region, Central Asia, *J. Geophys. Res.*, *100*, 20,321–20,343, 1995.

Matte, P., P. Tapponnier, N. Arnaud, L. Bourjot, J. P. Avouac, P. Vidal, Q. Liu, Y. Pan, and Y. Wang, Tectonics of western Tibet, between the Tarim and the Indus, *Earth Planet. Sci. Lett*, *142*, 311–330, 1996.

McCaffrey, R., Oblique plate convergence, slip vectors, and forearc deformation, *J. Geophys. Res.*, *97*, 8905–8915, 1992.

McCaffrey, R., Global variability in subduction thrust zone-forearc systems, *Pure Appl. Geophys.*, *142*, 173–224, 1994.

McCaffrey, R., Estimates of modern arc-parallel strain rates in fore arcs, *Geology*, *24*, 27–30, 1996.

Molnar, P., and W.-P. Chen, Seismicity and mountain building, in *Mountain Building Processes*, edited by K. Hsü, pp. 41–57, Academic, San Diego, Calif., 1982.

Molnar, P., and P. Tapponnier, Cenozoic tectonics of Asia: Effects of a continental collision, *Science*, *189*, 419–426, 1975.

Molnar, P., and P. Tapponnier, Active tectonics of Tibet, *J. Geophys. Res.*, *83*, 5361–5375, 1978.

Nábelek, J. L., Determination of earthquake source parameters from inversion of body waves, Ph.D. thesis, Mass. Inst. of Technol., Cambridge, 1984.

Ouchi, T., and H. Kawakami, Microseismicity in the middle Okinawa trough, *J. Geophys. Res.*, *94*, 10,601–10,608, 1989.

Pezzopane, S. K., and S. G. Wesnousky, Large earthquakes and crustal deformation near Taiwan, *J. Geophys. Res.*, *94*, 7250–7264, 1989.

Rau, R.-J., 3-D seismic tomography, focal mechanisms, and Taiwan orogeny, Ph.D. thesis, State Univ. of N. Y. at Binghamton, 1996.

Rau, R.-J., and F. T. Wu, Tomographic imaging of lithospheric structures under Taiwan, *Earth Planet Sci. Lett.*, *133*, 517–532, 1995.

Salzberg, D. H., Simultaneous inversion of moderate earthquakes using body and surface waves: Methodology and applications to the study of the tectonic of Taiwan, Ph.D. thesis, State Univ. of N. Y. at Binghamton, 1995.

Sato, T., S. Koresawa, Y. Shiozu, F. Kusano, S. Uechi, O. Nagaoka, and J. Kasahara, Microseismicity of back-arc rifting in the middle Okinawa Trough, *Geophys. Res. Lett.*, *21*, 13–16, 1994.

Seno, T., S. Stein, and A. E. Gripp, A model for the motion of the Philippine Sea Plate consistent with NUVEL-1 and geological data, *J. Geophys. Res.*, *98*, 17,941–17,948, 1993.

Shiono, K., T. Mikumo, and Y. Ishikawa, Tectonics of the Kyushu-Ryukyu Arc as evidenced from seismicity and focal mechanism of shallow to intermediate-depth earthquakes, *J. Phys. Earth*, *28*, 17–43, 1980.

Sibuet, J.-C., J. Letouzey, F. Barbier, J. Charvet, J.-P. Foucher, T. W. C. Hilde, M. Kimura, C. Ling-Yun, B. Marsset, C. Muller, and J.-F. Stephan, Back arc extension in the Okinawa trough, *J. Geophys. Res.*, *92*, 14,041–14,063, 1987.

Song, D.-R., K.-F. Ma, and L.-G. Liu, Rheological model in Taiwan: Constraints from geotherm and composition, in *Proceedings of the 1997 Annual Meeting of the Geological Society of China*, , pp. 366–368, Geol. Soc. of China, Tainan, 1997.

Suppe, J., A retrodeformable cross section of northern Taiwan, *Proc. Geol. Soc. China*, *23*, 46–55, 1980.

Suppe, J., Mechanics of mountain building and metamorphism in Taiwan, *Mem. Geol. Soc. China*, *4*, 67–89, 1981.

Suppe, J., Kinematics of arc-continent collision, flipping of subduction, and back-arc spreading near Taiwan, *Mem. Geol. Soc. China*, *6*, 21–33, 1984.

Tapponnier, P., G. Peltzer, A. Y. L. Dain, and R. Armijo, Propagating extrusion tectonics in Asia: New insights from simple experiments with plasticine, *Geology*, *10*, 611–616, 1982.

Teng, L. S., Geotectonic evolution of late Cenozoic arc–continent collision, *Tectonophysics*, *183*, 57–76, 1990.

Tsai, C.-S., M.-D. Lin, and Y.-B. Tsai, Relocation of the 12 March 1966 earthquake sequence in northeast Taiwan offshore, *Open Rep. ASIES-CR8306*, Inst. of Earth Sci., Acad. Sin., Taipei, 1983.

Tsai, Y.-B., Seismotectonics of Taiwan, *Tectonophysics*, *125*, 17–37, 1986.

Tsai, Y.-B., and S.-H. Wu, On the earthquake mislocation error due to the geometrical distribution of seismograph stations in Taiwan, in *Proceedings of the Symposium on Taiwan Strong Motion Instrumentation Program (II)*, pp. 178–186, Cent. Weather Bur., Taipei, 1996.

Vilotte, J. P., M. Daignieres, and R. Magariaga, Numerical modeling of intraplate deformation: Simple mechanical models of continental collision, *J. Geophys. Res.*, *87*, 10,709–10,728, 1982.

Wadati, K., Existence and study of deep earthquakes (in Japanese), *J. Meteorol. Soc. Jpn.*, *Ser. 2*, *5*, 119–145, 1927.

Wang, C.-Y., A. Ellwood, F. Wu, R.-J. Rau, and H.-Y. Yen, Mountain-building in Taiwan and the critical wedge model, in *Subduction Top to Bottom*, edited by G.E. Bebout, D.W. Scholl, S.H. Kirby, and J.P. Platt, pp. 49–55, AGU, Washington, D. C., 1996.

Wang, J.-H., K.-C. Chen, and T.-Q. Lee, Depth distribution of shallow earthquakes in Taiwan, *J. Geol. Soc. China*, *37*, 125–142, 1994.

Wu, F. T., Recent tectonics of Taiwan, *J. Phys. Earth*, *26*, suppl., S265–S299, 1978.

Wu., F., R.-J. Rau, and D. Salzberg, Taiwan orogeny: Thin-skinned or lithospheric collision, *Tectonophysics*, *274*, 191–220, 1997.

Yamono, M., S. Uyeda, Y. Furukawa, and G. A. Dehghani, Heat flow measurements in the northern and middle Ryukyu arc area on R/V *Sonne* in 1984, *Bull. Earthquake Res. Inst. Univ. Tokyo*, *61*, 311–327, 1986.

Yeh, Y.-H., C.-H. Lin, and S. W. Roecker, A study of upper crustal structures beneath northeastern Taiwan: Possible evidence of the western extension of Okinawa trough, *Proc. Geol. Soc. China*, *32*, 139-156, 1989.

H. Kao, Institute of Earth Sciences, Academia Sinica, P.O. Box 1-55, Nankang, Taipei, Taiwan. (e-mail: kao@earth.sinica.edu.tw)

K.-F. Ma and S. J. Shen, Institute of Geophysics, National Central University, Chung-Li, Taiwan.

(Received April 1, 1997; revised October 24, 1997;
accepted November 24, 1997.)